Portable neuroimaging guided non-invasive brain stimulation of cortico-cerebello-thalamo-cortical loop in substance use disorder

Pushpinder Walia[1], Abhishek Ghosh[2], Shubhmohan Singh[2], and Anirban Dutta[1*]

[1]Neuroengineering and Informatics for Rehabilitation Laboratory, University at Buffalo, Buffalo, NY, USA

[2]Postgraduate Institute of Medical Education & Research, Chandigarh, India.

*** Correspondence:**
anirband@buffalo.edu

Keywords: functional near-infrared spectroscopy; electroencephalogram; cortico-cerebello-thalamo-cortical loop; transcranial electrical stimulation; transcranial magnetic stimulation.

Abstract

Background: Maladaptive neuroplasticity related learned response in substance use disorder (SUD) can be ameliorated using non-invasive brain stimulation (NIBS); however, inter-individual variability needs to be addressed for clinical translation.

Objective: Our first objective was to develop a hypothesis for NIBS for learned response in SUD based on competing neurobehavioral decision systems model. Next objective was to conduct computational simulation of NIBS of cortico-cerebello-thalamo-cortical (CCTC) loop in cannabis use disorder (CUD) related dysfunctional "cue-reactivity" – a closely related construct of "craving" that is a core symptom. Our third objective was to test the feasibility of our neuroimaging guided rational NIBS approach in healthy humans.

Methods: "Cue-reactivity" can be measured using behavioral paradigms and portable neuroimaging, including functional near-infrared spectroscopy (fNIRS) and electroencephalogram (EEG), metrics of sensorimotor gating. Therefore, we conducted computational simulation of NIBS, including transcranial direct current stimulation(tDCS) and transcranial alternating current stimulation(tACS) of the cerebellar cortex and deep cerebellar nuclei(DCN), of the CCTC loop for its postulated effects on fNIRS and EEG metrics. We also developed a rational neuroimaging guided NIBS approach for cerebellar lobule (VII) and prefrontal cortex based on healthy human study.

Results: Simulation study of cerebellar tDCS induced gamma oscillations in the cerebral cortex while tTIS induced gamma-to-beta frequency shift. Experimental fNIRS study found that 2mA cerebellar tDCS evoked similar oxyhemoglobin(HbO) response in-the-range of $5x10^{-6}$M across cerebellum and PFC brain regions (α=0.01); however, infra-slow (0.01–0.10 Hz) prefrontal cortex HbO driven(phase-amplitude-coupling, PAC) 4Hz, ±2mA (max.) cerebellar tACS evoked HbO in-the-range of 10^{-7}M that was statistically different (α=0.01) across those brain regions.

Conclusion: Our healthy human study showed the feasibility of fNIRS of cerebellum and PFC as well as fNIRS-driven ctACS at 4Hz that may facilitate cerebellar cognitive function via the frontoparietal network. Future work needs to combine fNIRS with EEG for multi-modal imaging.

1 Introduction

Neurobiological framework from misusing addictive drugs to substance use disorder (SUD) is increasingly shown to be related to neuroplastic changes in the structure and function that promote and sustain SUD, including addiction – the most severe form of SUD (Administration (US) and General (US), 2016). Onset, development, and maintenance of SUD show dysfunction in three main areas of the brain; the basal ganglia, the extended amygdala, and the prefrontal cortex (Administration (US) and General (US), 2016). Brain dysfunction can trigger different behavioral aspects of SUD, including substance-seeking triggered by substance-associated cues, reduced sensitivity to reward and heightened activation of brain stress systems, and reduced executive control. Here, adolescence is a critical "at-risk period" for all addictive drugs, including alcohol and cannabis, where neuroplastic changes due to a less potent drug may facilitate substance-seeking of a more potent addictive drug. The differential nature of the interactions between the substance use and brain structure maturation across adolescence and into young adulthood has been highlighted in a recent work (Windle et al., 2018).

Cannabis is the most widely cultivated, trafficked, and abused illicit drug (WHO | Cannabis; World Drug Report 2020). In 2018, an estimated 192 million people aged 15-64 years used cannabis for nonmedical purposes globally (Degenhardt et al., 2013). The Global Burden of Diseases, Injuries, and Risk Factors Study (GBD) 2016 estimated that, across the globe, there were more than 22.1 million people with cannabis dependence (Degenhardt et al., 2018). Moreover, the same study calculated that cannabis dependence could be accounted for 646 thousand Disability Adjusted Life Years globally. Significantly, cannabis dependence mainly affects young adults (20-24 years), which has a significant negative impact on these individuals' growth and productivity and the societies and nations (Degenhardt et al., 2013). In addition to the dependence syndrome, cannabis use is associated with an increased risk of psychosis (Large et al., 2011), cognitive dysfunction, academic problems, and roadside accidents (Volkow et al., 2014). A review showed a consistent association between cannabis use and lower educational attainment and increased reported use of other illicit drugs (Macleod et al., 2004). In the United States, Cannabis Use Disorder (CUD) is an escalating problem in young adults by legalization (Cerdá et al., 2020) where National Survey on Drug Use and Health reported increased prevalence from 5.1% in 2015 to 5.9% in 2018 in 18-25-year-olds (2019 NSDUH Detailed Tables | CBHSQ Data).

The psychoactive effects are primarily due to type 1 cannabinoid receptor (CB1), the cannabinoid binding protein, that is highly expressed in the cerebellar cortex (Marcaggi, 2015). CB1 is primarily found in the molecular layer at the most abundant synapse type in the cerebellum (Marcaggi, 2015) that can shape the spike activity of cerebellar Purkinje cell (Brown et al., 2019). Moreover, granule cell to Purkinje cell synaptic transmission can trigger endocannabinoid release (Alger and Kim, 2011), which may be important for information processing by cerebellar molecular layer interneurons (Dorgans et al., 2019). This suggests that endocannabinoids could be essential to neurocognitive aspects of cerebellar function (Di Marzo et al., 2015),(Marcaggi, 2015),(Alger and Kim, 2011), and CB1 receptor downregulation in long-term chronic cannabis use may promote CUD (Hirvonen et al., 2012). Accumulating evidence also suggests cerebellar modulation of the reward circuitry and social behavior via direct cerebellar innervation of the ventral tegmental area (VTA), including dopamine cell bodies (A1) in the VTA (Carta et al., 2019). The VTA-dopamine (DA) signaling in the nucleus accumbens (NAc) and the medial prefrontal cortex (MPFC) (Lohani et al., 2019) play a crucial role in motivated behavior and cognition. Cerebellar neuropathological changes can result in aberrant dopaminergic activity in the NAc and MPFC (ROGERS et al., 2011),(Lohani et al., 2019) leading to dysfunctional behavior and cognition. Therefore, there is a critical need to determine how the cerebellum modulate limbic VTA-DA signaling since endocannabinoid system is

Preprints (www.preprints.org) | NOT PEER-REVIEWED | Posted: 4 January 2022 doi:10.20944/preprints202201.0008.v1

essential to cerebellar function. Here, CUD related cerebellar dysfunction is postulated that can include reward-related behaviors, information processing, and cognitive control (Di Marzo et al., 2015),(Marcaggi, 2015),(Alger and Kim, 2011).

NIBS based on competing neurobehavioral decision systems model

Research on repetitive Transcranial Magnetic Stimulation (rTMS) for the treatment of substance dependence showed encouraging results so far, especially concerning the reduction of craving for drug use and improving cognitive outcomes (Makani et al., 2017)(Ekhtiari et al., 2019; Stein et al., 2019). However, NIBS's effect is only transient and fades rapidly after treatment termination (Stein et al., 2019). Craving is postulated as the failure of the normal inhibitory processes mediated by prefrontal cortex (PFC) regions to control reward processes mediated by the limbic system (Goldstein and Volkow, 2011). Although neuroimaging studies have implicated diverse PFC regions; however, the right inferior frontal cortex has been implicated mainly by the human lesion-mapping (Aron et al., 2004). Therefore, excitatory rTMS to the executive control network (dorsolateral prefrontal cortex – DLPFC)(Sahlem et al., 2018) or inhibitory rTMS to the reward network can be postulated to result in decreased craving. Indeed, left DLPFC is the most frequent anatomical target in clinical studies, followed by right DLPFC (Ekhtiari et al., 2019). Here, excitatory rTMS at the left DLPFC has shown activation of the executive control network to reduce craving in substance use disorders (Claire Wilcox, 2019). Figure 1 shows the cerebellocortical circuit for our competing neurobehavioral decision systems (CNDS) approach for planning NIBS intervention that depends on the delineation of the functional organization of prefrontal cortex (Levy and Wagner, 2011) for portable neuroimaging guided NIBS (Walia et al., 2021). The activation of executive control network via DLPFC for the relative inhibition of the frontal–striatal circuits involved in limbic (amygdala, nucleus accumbens, ventral pallidum, and related structures) reward while activation of the ventrolateral prefrontal cortex (VLPFC) can facilitate the cognitive control of memory (Badre and Wagner, 2007). Here, the inferior frontal gyrus (IFG) in the VLPFC (Barredo et al., 2016) is postulated to be crucial for memory retrieval (IFG pars orbitalis) (Torregrossa et al., 2011) and post-retrieval control processes for amplifying the downstream inhibition from the subthalamic nucleus (Rae et al., 2015) when substance-seeking is triggered by substance-associated cues (Chambers et al., 2006). Dysfunctional response inhibition system following substance-associated cues are postulated to trigger “automatic” goal-directed substance-seeking behavior where distinct neural circuits are responsible for the acquisition (during drug misuse) and “automatic” performance of the “learned” behavior (in SUD, addiction). Goal-directed behaviors are driven by brain structures including the medial prefrontal and orbitofrontal cortices, hippocampus, ventral and dorsomedial striatum, while sensorimotor cortices and dorsolateral striatum mediate the automatized/reflexive behavior. Within this brain network, the dorsomedial striatum (DMS) receives excitatory inputs from PFC, whereas the dorsolateral striatum (DLS) primarily receives inputs from the sensorimotor and premotor cortices. In primates, the caudate nucleus and the putamen correspond to the DMS and DLS in rodents, where DLS has been shown to mediate stimulus-response habits (Balleine and O’Doherty, 2010). This network mapping can be related to habitual performance, i.e. when the response is no longer adaptive (Vandaele et al., 2019). Animal studies have shown distinct DMS and DLS activity patterns during the early acquisition stage and become similar during an automatized performance. Extinction learning may enable learning of new contingencies via inhibition of the automatized response that will require facilitation of the inhibitory connections from the PFC to the subcortical regions to enable cognitive flexibility (Haluk and Floresco, 2009; Myers and Carlezon Jr., 2010). Here, a cortical-dorsomedial striatal circuit starting from PFC is responsible for acquiring goal-directed actions while a cortical-ventral striatal circuit mediates the performance (Balleine and O’Doherty, 2010). Therefore, it is postulated that the response inhibition system can be facilitated by the activation of IFG for proactive control (Chambers et al., 2006; Leite et al., 2018) during cue-

Preprints (www.preprints.org) | NOT PEER-REVIEWED | Posted: 4 January 2022 doi:10.20944/preprints202201.0008.v1

exposure therapy (Hone-Blanchet et al., 2014), where a decrease in ventral striatum activity has been shown to correlate with the treatment effects (Schacht et al., 2013).

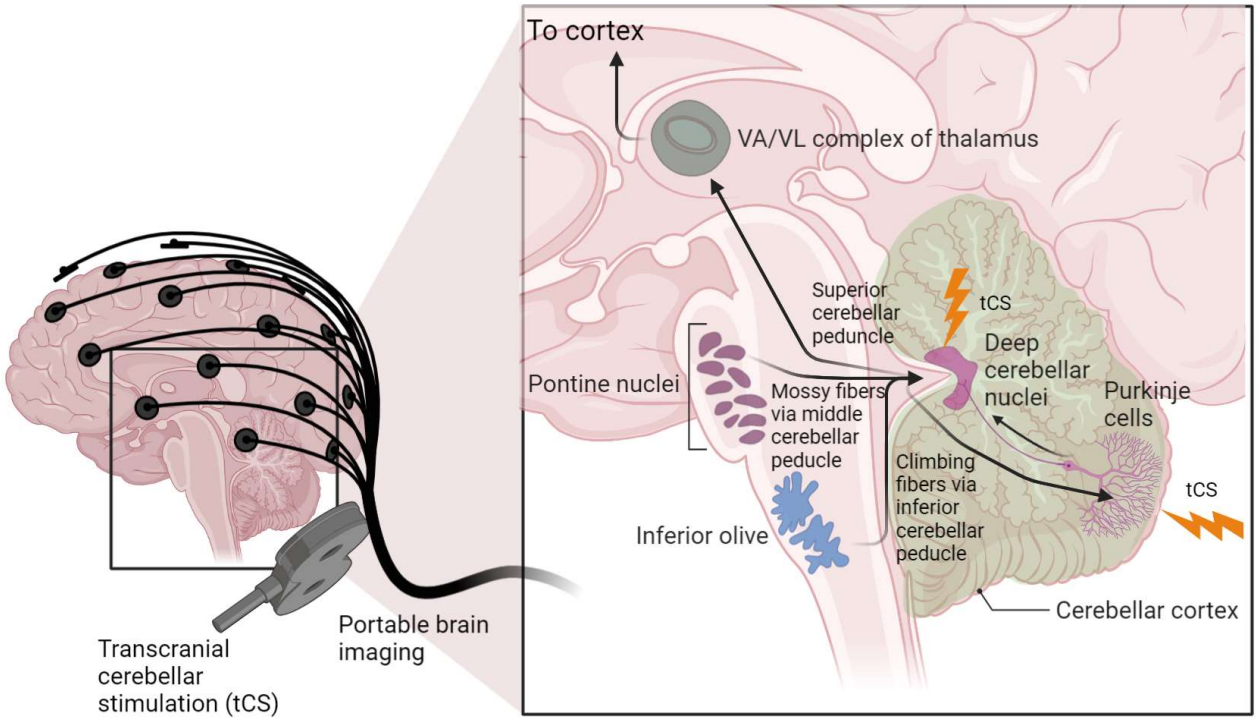

Figure 1: Cerebellocortical circuit. Cerebellum sends its output through the superior cerebellar peduncle, the contralateral red nucleus, and ventral anterior/ventral lateral nucleus of the thalamus to various cerebral areas including the motor cortex, the prefrontal cortex, the parietal cortex, and the temporal cortex. Recent work found that frontoparietal network is disproportionately expanded in the cerebellum compared to cortex. Transcranial cerebellar stimulation can affect the integration of the sensory and the cortical signals at the cerebellar cortex (Purkinje cells) as well as the deep cerebellar nuclei through which the cerebellum delivers its output to the cerebral cortex.

In this study, we review NIBS methods to reduce "craving" – a core symptom of SUD; however, defining "craving" is challenging (Ekhtiari et al., 2019). Therefore, "cue-reactivity" is used as a closely related construct that can be measured using behavioral paradigms and imaging metrics (e.g., electroencephalogram, functional brain imaging, eye-tracking/pupilometry, heart rate) (Ekhtiari et al., 2019). Besides medial prefrontal cortex (MPFC) and cingulate cortex, which may predict relapse across multiple substances (Ekhtiari et al., 2019), we postulate that the cerebellum may also modulate the allocation of the attentional resources (Mannarelli et al., 2019) to cue stimuli relevant in "cue-reactivity." Specifically, the default mode network, based in ventromedial prefrontal cortex (vmPFC) and posterior cingulate cortex (PCC) (Uddin et al., 2009), may directly modulate "cue-reactivity" in relapse for task-positive networks for substance-seeking. Whole-brain network studies show that cerebellum and striatum are functionally connected with the cortical regions of the default mode network (Alves et al., 2019) that needs further elucidation. Then, recent work found that frontoparietal network is disproportionately expanded in the cerebellum compared to cortex (Marek et al., 2018). Therefore, cerebellar NIBS may facilitate attentive executive function (Mannarelli et al., 2019) in the Posnerian model to reduce "cue-reactivity." Here, portable imaging metrics from eye-tracking (Kumar et al., 2016), electroencephalogram (EEG) (Mannarelli et al., 2020), and functional near-infrared

Preprints (www.preprints.org) | NOT PEER-REVIEWED | Posted: 4 January 2022 doi:10.20944/preprints202201.0008.v1

spectroscopy (fNIRS) (Huhn et al., 2019) can provide insights into NIBS effects during a "cue-reactivity" test that can be less challenging at the point-of-care settings than functional magnetic resonance imaging (fMRI) (Cousijn et al., 2013). Here, EEG delta power has been postulated to be linked to increased activity of the dopaminergic brain reward system (Wacker et al., 2009) and increased craving (Pripfl et al., 2014) so reduced EEG delta power can be related to therapeutic benefit.

Multi-modal portable fNIRS-EEG joint-imaging (Sood et al., 2016) is postulated to capture the subject-specific response for dosing NIBS. Here, inhibition of the reward network is postulated to be achieved by cerebellar rTMS (Fernandez et al., 2020) via cerebellar innervation of the dopamine cell bodies in the VTA (Carta et al., 2019). Low-intensity rTMS is proposed to primarily affect the Purkinje cells in the cerebellum (Morellini et al., 2015) that is GABA-mediated inhibition of the deep cerebellar nuclei (DCN) in the fronto-cerebellar circuit (Middleton and Strick, 2001). We augmented the CNDS theory (Koffarnus et al., 2013) (Hanlon et al., 2018) with recent evidence from neuroimaging studies that fronto-cerebellar circuit, which interacts with brain's default mode network, is relevant in cognitive functions (ROGERS et al., 2011), and that cognitive control (Zhang and Volkow, 2019) may be diminished in the addicted brain with memory, reward/saliency, and motivation/drive components (Moulton et al., 2014). Therefore, it may be possible to exert a longer term effect via cerebellar NIBS because of its broader connections with the memory circuit and the role in habit formation (Moulton et al., 2014). In fact, animal studies have shown cerebellar contribution to extinction learning where the motor memory preserved in the cerebellum needs to be inhibited by the forebrain structures via the amygdala complex (Hu et al., 2015). Therefore, neuroplastic changes at the cerebellum is postulated to be crucial for long-term therapeutic effects by reducing cerebellar "addiction" memory (lobule VIIb (Moulton et al., 2014)). Indeed, human study showed detrimental effect of anodal cerebellar tDCS on the performance and timing of learned motor responses; however, the extinction learning was not affected during the acquisition phase (Kimpel et al., 2020). Here, effects on motor learning can provide important insights since motor symptoms can be a characteristic of the disorder (Walther and Strik, 2012). Based on these prior works, we postulate lobule VII (including Crus I, Crus II, and lobule VIIb) specific cerebellar NIBS (Rezaee and Dutta, 2019),(Rampersad et al., 2014) to facilitate extinction learning toward substance-related cues in CUD.

Relevance of cerebellar NIBS in cannabis use related psychotic disorder

Targeting maladaptive plasticity in the cerebellum was considered crucial due to significant FGFR1 and AKT1 gene expression, as shown in Figure 2. FGFR1 possesses mechanisms to activate the Akt signaling pathway relevant in neurodevelopment in schizophrenia (Zheng et al., 2012). Here, protein kinase Akt1's role in dopamine neurotransmission has been implicated in schizophrenia and psychosis (Shumay et al., 2017). FGF21 has been found to regulate sweet and alcohol preference that correlated with reductions in dopamine concentrations in the nucleus accumbens, which coordinates reward behavior (Talukdar et al., 2016). Interestingly, excitation/inhibition (E/I) balance is disrupted in schizophrenia (Dutta et al., 2020) that can affect the prefrontal cortex (Page and Coutellier, 2018) and cerebellum (Gao and Penzes, 2015) leading to substance abuse (Winklbaur et al., 2006) in adolescence. In the cerebellum, the only output from the cerebellar cortex is represented by the inhibitory GABAergic Purkinje cells (Hirano, 2013), while CB1 receptors are mainly expressed in the presynaptic terminals of granule cells molecular layer interneurons, and climbing fibers that synapses onto Purkinje cells. Here, CB1 receptor activity is required for long-term plasticity at parallel fiber-Purkinje cells synapses relevant for cerebellar learning. CB2 receptors in Purkinje cells may mainly participate in pathophysiological responses to exogenous cannabinoid compounds that can inhibit GABA receptor-mediated currents potentially causing cerebellar dysfunction (Sadanandan et al., 2020). This will reduce the inhibitory tone the cerebellum that can be investigated based on the primary

Preprints (www.preprints.org) | NOT PEER-REVIEWED | Posted: 4 January 2022 doi:10.20944/preprints202201.0008.v1

motor cortex, i.e., CBI, that can be impaired in CUD (Martin-Rodriguez et al., 2020) and schizophrenia (Walther and Strik, 2012). Therefore, ameliorating maladaptive neuroplasticity in the cerebellum using NIBS is crucial in CUD since brain-wide AKT1 and FGFR1 gene expressions show hot-spot at the cerebellum, as shown in Figure 2 (from https://neurosynth.org/), which makes it relevant for progression to psychotic disorder especially with genetic predisposition (Power et al., 2014). In fact, AKT1 genotype has been shown to influence the risk of psychosis, especially in young cannabis users (Di Forti et al., 2012). Also, an altered function of fibroblast growth factor receptors (FGFR) signaling can be associated (Klejbor et al., 2009) where FGFR uses endocannabinoid signaling system during neurodevelopment (Williams et al., 2003). Here, FGF7 and FGF22 have been shown to differentially promote the formation of inhibitory or excitatory presynaptic terminals (Brewer et al., 2016) that may play a role in E/I balance (Gao and Penzes, 2015).

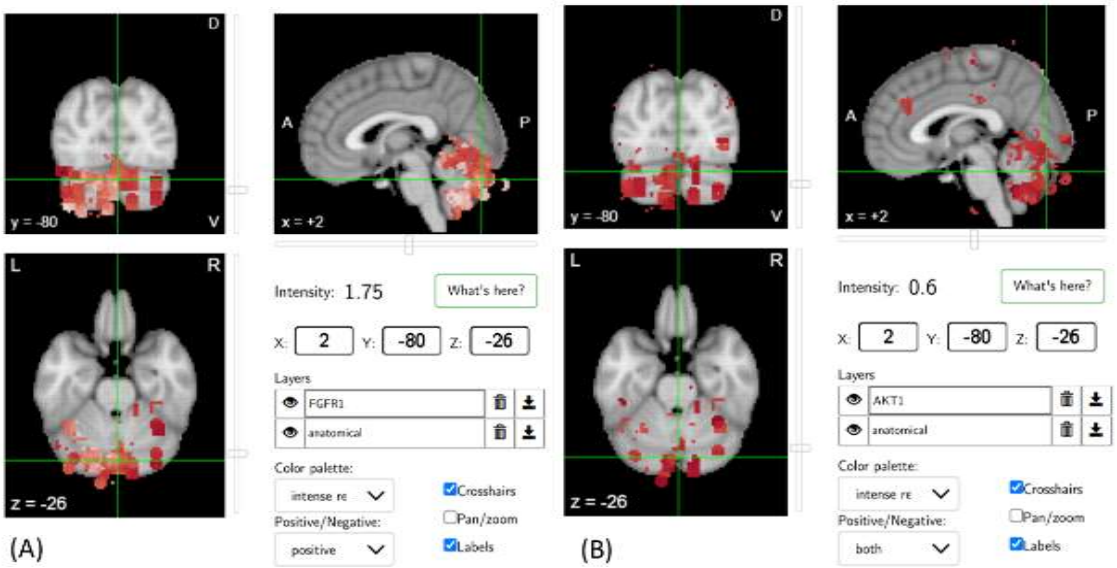

Figure 2: Brain-wide gene expression level of gene FGFR1 (A) and AKT1 (B) as made available from Allen Human Brain Atlas (from https://neurosynth.org/).

Cerebellar NIBS can facilitate amelioration of CUD related maladaptive plasticity as an adjuvant treatment to cognitive control training during a visual cue-reactivity paradigm using a virtual reality (VR) interface. Specifically, transcranial electrical stimulation (tES), a NIBS modality, is translatable to low-cost (<$150) mobile devices that can allow remote delivery of cerebellar NIBS in conjunction with VR-based cognitive training in a low resource home-based setting (Carvalho et al., 2018). In this methodological study, we aim to address dysfunctional sensory/sensorimotor gating, including prepulse inhibition, found to be deficient in chronic cannabis use (Kedzior and Martin-Iverson, 2006) and schizophrenia (Rohleder et al., 2016). A recent work found that the frontoparietal network involved in executive function and goal-oriented behavior is disproportionately expanded in the cerebellum compared to cortex (Marek et al., 2018). Furthermore, Marek et al. (Marek et al., 2018) found that cerebellar blood-oxygen-level-dependent imaging signals temporally lag the cortex where the infra-slow activity (0.01–0.10 Hz) and delta band (0.5–4 Hz) activity propagated in opposite directions between the cerebellum and cerebral cortex. Therefore, tES with transcranial direct current stimulation (tDCS) and transcranial alternating current stimulation (tACS) were investigated for neuromodulation of the cerebellum and cerebral cortex with computational simulations. Here, tES applied low currents around 2mA that generated cortical electric fields less than 1 V/m (Huang et al., 2017), which has shown entrainment effects in the case of tACS (Johnson et al., 2020). We present the combined functional near-infrared spectroscopy (fNIRS) and electroencephalogram (EEG) approach to monitor

Preprints (www.preprints.org) | NOT PEER-REVIEWED | Posted: 4 January 2022 doi:10.20944/preprints202201.0008.v1

and dose tES, including entrainment effects, based on prior works (Sood et al., 2016),(Guhathakurta and Dutta, 2016),(Dutta et al., 2015),(Rezaee et al., 2021). This is crucial in SUD since both inter-individual variability in genetics and environment influence schizophrenia, a neurodevelopmental disease with a delayed post-pubertal onset (Klejbor et al., 2009). We conducted a feasibility testing of fNIRS in young and healthy subjects to drive (phase amplitude coupling) cerebellar tACS (ctACS) at 4Hz using infra-slow (0.01–0.10 Hz) PFC oxyhemoglobin concentration changes (HbO). Here, fNIRS-driven 4Hz ctACS at ±2mA (max.) is expected to facilitate cerebellar brain inhibition (Spampinato et al., 2021) better than 2mA cerebellar tDCS (ctDCS) based on fNIRS imaging (Rezaee et al., 2021).

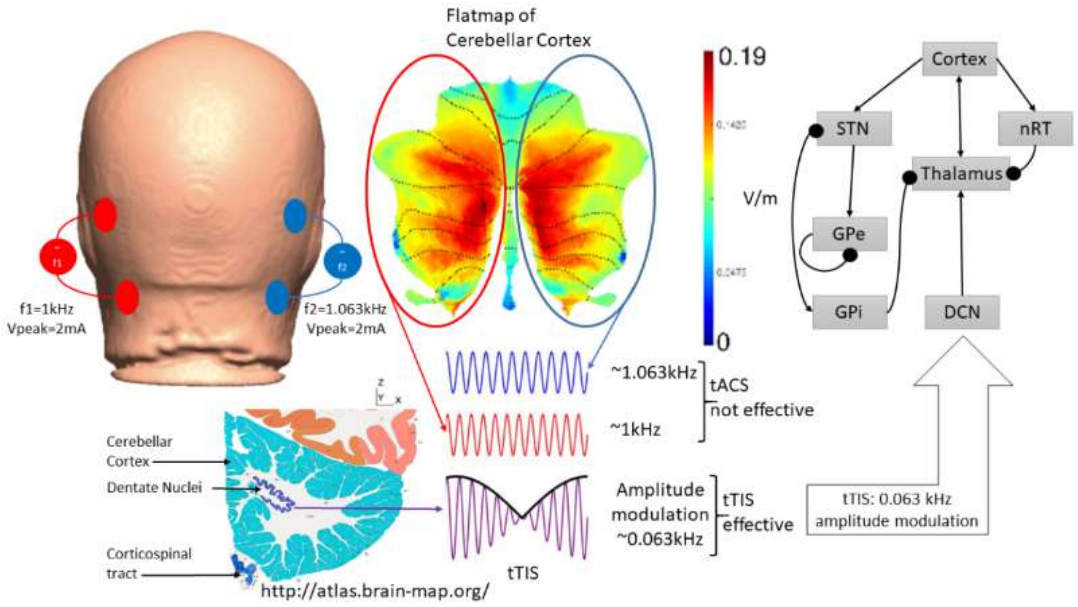

Figure 3: An illustration of postulated transcranial temporal interference stimulation (tTIS) approach for deep cerebellar NIBS where two tACS sources with frequencies f1=1kHz and f2=1.063kHz are combined for amplitude modulation at 0.063kHz at the deep cerebellar nuclei (DCN) regions. The thalamocortical basal ganglia network with DCN from (Yousif et al., 2020) is presented for tTIS modeling where arrows denote excitatory connections and round arrowheads denote inhibitory connections.

2 Methods

We postulate NIBS based amelioration of dysrhythmia in the cortico-cerebello-thalamo-cortical (CCTC) loop as an extension to thalamocortical dysrhythmia (Schulman et al., 2011). We investigated transcranial temporal interference stimulation (tTIS) approach (Lee et al., 2020) using a CCTC loop model (Zhang and Santaniello, 2019) that considered the average firing rate of the Purkinje cells (PCs) and deep cerebellar neurons (DCN) as 63Hz and 56.6Hz, respectively. So, for computational modeling of thalamocortical basal ganglia with cerebellum (Yousif et al., 2020), we selected f2-f1=63Hz for the amplitude modulation of DCN by tTIS (Grossman et al., 2017) – see Figure 3 (details in Supplementary materials). Thalamocortical basal ganglia model with cerebellum (Yousif et al., 2020) integrated two thalamic populations, the excitatory ventralis intermedius (Vim) nucleus and the inhibitory reticular nucleus (nRT), with an excitatory population of the deep cerebellar nuclei (DCN), an excitatory population representing the subthalamic nucleus (STN), and two inhibitory populations representing the external part of the globus pallidus (GPe) and the internal part of the globus pallidus (GPi), as shown in Figure 3. The model consisted of seven first-order coupled differential equations that

Preprints (www.preprints.org) | NOT PEER-REVIEWED | Posted: 4 January 2022 doi:10.20944/preprints202201.0008.v1

simulated the gamma-band oscillations (>30 Hz) for a constant external input to the DCN (details in Supplementary materials). It is postulated that this PCs modulation of DCN may be dysfunctional in CUD that can be related to increased risk of psychosis and schizophrenia with familial/genetic risk factors (Kuepper et al., 2011; Large et al., 2011; Kendler et al., 2015), e.g., increased CB1 expression (Marcaggi, 2015),(Alger and Kim, 2011) in the molecular layer (Marcaggi, 2015) can shape the spike activity of Purkinje cell (Brown et al., 2019). In CUD, a decrease in Purkinje cell density (Bernard and Mittal, 2014) can lead to dysrhythmia in the CCTC loop where increasing the residual Purkinje cell excitability with NIBS may ameliorate the dysrhythmia. Also, prior work (Hong et al., 2004) has identified gamma-to-beta frequency shift as a marker of sensory gating that was found deficient in schizophrenia. Additionally, previous results have shown that gamma and beta frequency oscillations occur in the neocortex in response to sensory stimuli over various modalities (Haenschel et al., 2000). Therefore, portable neuroimaging of the cerebellar tES response with combined fNIRS-EEG may guide the tES dosing based on general linear modeling of dose-response (Rezaee et al., 2021).

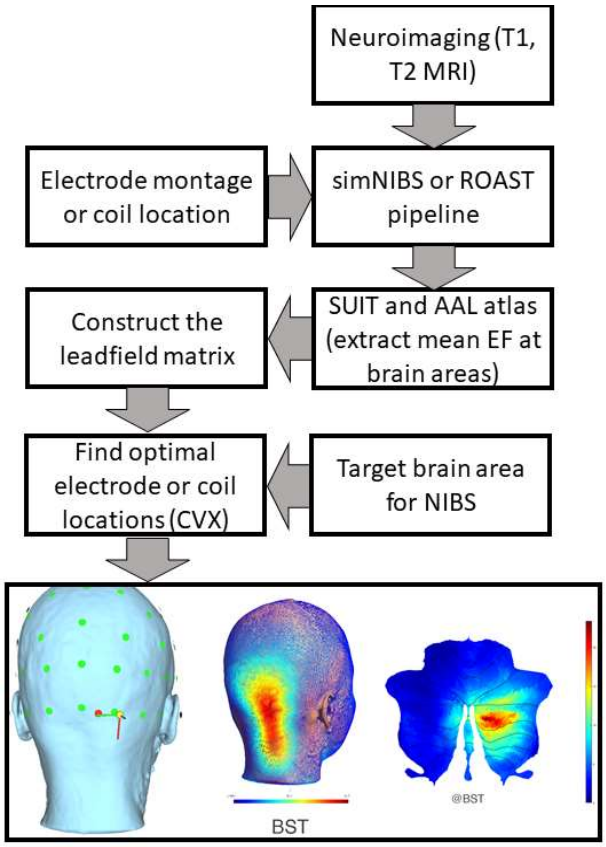

Figure 4: Computational pipeline for MRI based optimization of non-invasive brain stimulation for a target electric field (EF) distribution using convex optimization (CVX). Bottom panel shows an illustrative example of TMS targeting Crus II at brainstem threshold (@BST).

2.1 Neuroimaging guided non-invasive brain stimulation

Human functional neuroimaging has shown segregated fronto-cerebellar circuits (Krienen and Buckner, 2009), e.g., DLPFC-correlated activity was shown to span cerebellar Crus I/II lobules in its lateral and ventral extent. In contrast, MPFC-correlated activity spanned cerebellar Crus I lobule. Here, Crus I preferentially correlated with MPFC while Crus II preferentially correlated with DLPFC. Such lobule-specific rTMS will require a neuroimaging guided individualized approach with a Cerebellar Lobules Optimal Stimulation (CLOS) pipeline (Figure 4) for the delivery of neuroimaging guided

Preprints (www.preprints.org) | NOT PEER-REVIEWED | Posted: 4 January 2022 doi:10.20944/preprints202201.0008.v1

cerebellar NIBS – details in the Supplementary materials based on our prior works (Rezaee and Dutta, 2019). In this study, we investigated the "knee" in the recruitment of the cerebellar-primary motor cortex (M1) connection, or the cerebellar-brain inhibition (CBI) recruitment curve, at different intensities of the cerebellar TMS conditioning stimulus based on computational modeling and published experimental results (Batsikadze et al., 2019). In a feasibility study (Rezaee et al., 2021), we hypothesized that the combination of fNIRS and EEG would allow for non-invasive and simultaneous assessment of cerebral response to bilateral deep ctDCS of the dentate nucleus (DN) and cerebellar lobules VII-IX. Here, ctDCS was optimized for targeting the dentate nucleus (Rezaee et al., 2020a) that stimulated anterior and posterior lobes of the cerebellum, including cerebellar hemispheric lobules Crus I–Crus II and the dentate nucleus (Rezaee et al., 2020a), which was postulated to modulate the cerebrum activity differently than ctDCS of the posterior lobes of the cerebellum consisting of the hemispheric lobules VIIb-IX. The top panel of the Figure 1 shows the cerebellocortical circuit where cerebellar NIBS can be targeted not only at the cerebellar cortex, including Purkinje cells that integrates sensory and cortical information (Walter and Khodakhah, 2006), but also the dentate nuclei through which the cerebellum delivers its vast amount of output to the cerebral cortex (Ishikawa et al., 2014).

Table 1: Subject details (all male) for computational simulations using retrospective data (Rezaee et al., 2021)

Name	Age and age-group for CLOS (years)	Post Stroke Period (years)	Hemiplegic Side	Cerebellar tDCS (Anode-Cathode)
P1	44 (40-44)	2	Right	PO10h-PO9h
P2	53 (50-54)	3	Right	PO10h-PO9h
P3	40 (40-44)	1	Left	PO9h-PO10h
P6	50 (50-54)	2	Left	PO9h-PO10h
P7	61 (60-64)	1	Left	PO9h-PO10h

The research protocol was approved by the All India Institute of Medical Sciences, New Delhi, India Institutional Review Board (IEC-129/07.04.2017) and the Indian Institute of Technology Gandhinagar, India. We performed fNIRS-EEG joint-imaging covering the prefrontal cortex, the primary motor cortex, and the supplementary motor area to investigate the deep ctDCS effects on cerebrum activity. This was based on fMRI studies (Krienen and Buckner, 2009) that showed distinct PFC regions functionally connected to the multiple areas of the human cerebellum, e.g., Crus I with MPFC, Crus II with DLPFC. We applied a novel approach using latent variables from fNIRS and EEG using a general linear model (GLM) (Pinti et al., 2017) to study the effects of ctDCS. This was based on our prior works that showed ctDCS electrode montages could be optimized to stimulate different parts or lobules of the cerebellum (Rezaee and Dutta, 2019). Specifically, we found (Rezaee et al., 2021) that bilateral ctDCS of combined anterior and posterior lobes of the cerebellum, including cerebellar hemispheric lobules Crus I–Crus II and the dentate nucleus, resulted in increased canonical scores of oxy-hemoglobin (O2Hb) concentration changes as well as an increased canonical scores of

Preprints (www.preprints.org) | NOT PEER-REVIEWED | Posted: 4 January 2022 doi:10.20944/preprints202201.0008.v1

EEG from pre-ctDCS baseline at the contralateral (to the anode) PFC. In contrast, bilateral ctDCS of the hemispheric lobules VIIb-IX resulted in a small decrease in the canonical scores of O2Hb concentration changes and EEG from pre-ctDCS baseline at the contralateral PFC from pre-ctDCS baseline. Here, distinct areas of PFC are functionally connected to lobule VII of the cerebellum (Mannarelli et al., 2020), i.e., Crus I with MPFC, Crus II with DLPFC, ventral VIIB with anterior prefrontal cortex (APFC) (Rezaee et al., 2021). However, lesion heterogeneity led to inter-individual variability in the fNIRS-EEG response (Rezaee et al., 2021), so we selected best five subjects (Table 1) with the greatest post-ctDCS change in the canonical scores of O2Hb concentration from pre-tDCS baseline to determine their brain activation (Aasted et al., 2015a), as shown in Figure 5 (description in the supplementary materials). Open-source realistic volumetric-approach to simulate transcranial electric stimulation-ROAST pipeline (Huang et al., 2019) was used with maximal-focality optimization criteria to target the response inhibition brain activation with 4x1 high-definition (HD) tDCS montage (Mikkonen et al., 2020) – see Figure 5. The details are explained in the next subsections.

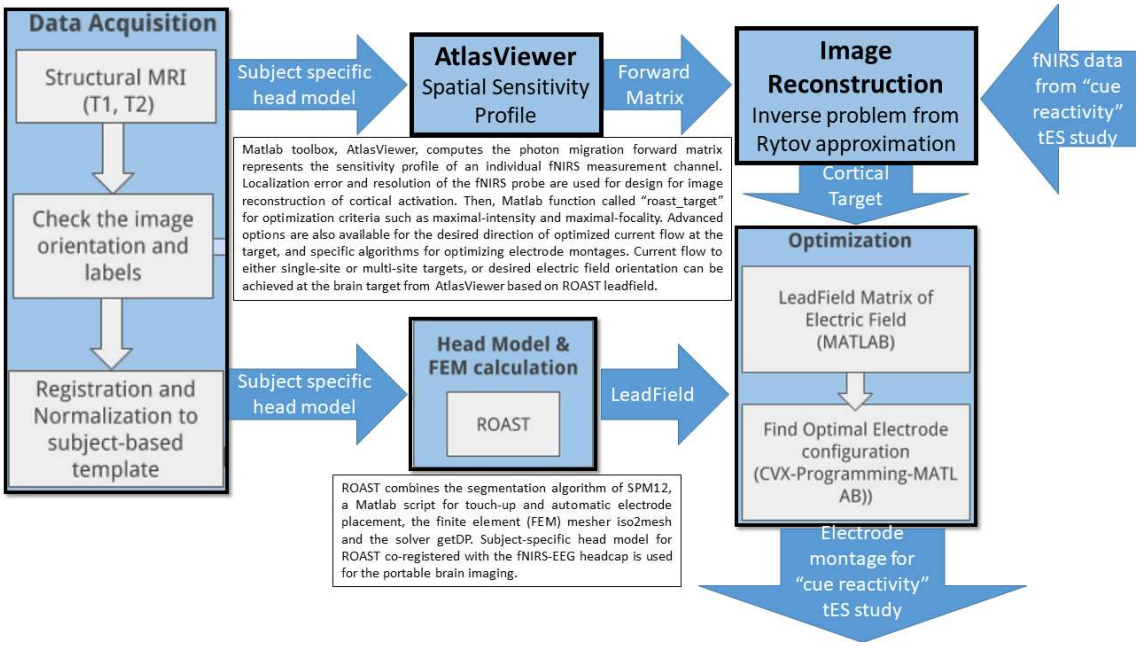

Figure 5: Computational pipeline for portable neuroimaging guided transcranial electrical stimulation.

2.1.1 fNIRS sensitivity profile for neuroimaging cerebellar NIBS in healthy humans

Individual head model was created based on structural magnetic resonance images (MRI) from our prior work on Cerebellar Lobules Optimal Stimulation (CLOS) pipeline (Rezaee and Dutta, 2019). MR images were taken from a young and healthy volunteer in accordance with the Declaration of Helsinki - a statement of ethical principles for medical research involving humans' study. The study was approved at the University at Buffalo, USA. Figure 5 shows neuroimaging guided transcranial electrical stimulation pipeline using subject-specific head model from SPM12 segmentation algorithm (https://www.fil.ion.ucl.ac.uk/spm/software/spm12/) in Matlab (Mathworks Inc., USA). CLOS pipeline can use realistic volumetric-approach to simulate transcranial electric stimulation—ROAST—pipeline (Huang et al., 2019) or, SimNIBS (Saturnino et al., 2018) for finite element analysis of the electric field for electrode optimization (Rezaee and Dutta, 2019),(Rezaee et al., 2020a). In our prior work, we have optimized bipolar ctDCS montage for lower-limb motor representations and dentate nuclei in case of stroke survivors (Rezaee et al., 2020a). Here, motor representations are twice whereas

Preprints (www.preprints.org) | NOT PEER-REVIEWED | Posted: 4 January 2022 doi:10.20944/preprints202201.0008.v1

non-motor representations (attentional/executive and default-mode) are thrice in each cerebellar cortical hemisphere (lobules VI-Crus I; lobules Crus II–VIIB; lobules IX–X) (Guell and Schmahmann, 2020). Three functional domains were found in the cerebellar cortex, i.e., the functional gradients in cerebellum, where Crus I/II intersection is the intersection of first and the second default-mode representation (Guell and Schmahmann, 2020). Viral tracing studies in non-human primates have shown Crus I/II to have projections only to the prefrontal cortex (Buckner et al., 2011). Also, functional MRI studies have shown Crus I connectivity with the MPFC while Crus II with the DLPFC (Krienen and Buckner, 2009). Therefore, in this study, we optimized electrode montage for the non-motor representation in the right cerebellar hemisphere, namely, right lobules VI-CrusI/II-VIIb, using CLOS pipeline (Rezaee and Dutta, 2019).

In our healthy human study, we compared ctACS and ctDCS effect based on fNIRS oxyhemoglobin concentration changes (HbO) at the prefrontal cortex (PFC), and cerebellum (CER). Session consisted of a block design of 3 min rest and ctDCS/ctACS duration of 5min which was chosen based on prior works that showed significant increase in the cortical excitability (Nitsche and Paulus, 2001) and cerebral blood flow changes (Paquette et al., 2011). Also, our computational modeling (Arora et al., 2021) showed feasibility of model linearization for evaluating the acute effects during first 150 seconds of primary motor cortex tDCS in healthy humans using fNIRS based measure of blood volume. We used the SPM12 segmented headmodel to run the freely available Monte-Carlo photon transport software (tMCimg) in the AtlasViewer (Aasted et al., 2015b) to compute fNIRS sensitivity profile based on our prior work (Guhathakurta and Dutta, 2016). Then, AtlasViewer (Aasted et al., 2015b) determined HbO hemodynamic response function to ctDCS/ctACS. The details of the study in the next subsection

2.1.2 fNIRS data acquisition and processing for the healthy human study

Ten young and healthy right-handed subjects (2 females, age: 21-25 years) volunteered for this study. The session consisted of a block design of 2.5 min baseline, ctDCS/ctACS period of 5min, and 2.5 min post-intervention measures. We postulated that the immediate tDCS effects on blood volume is mainly due to the pial vessels (sensitive to fNIRS) (Arora et al., 2021). In this healthy human study, fNIRS was conducted using NIRSPORT 2 (NIRx, USA) where our optode montage consisted of 12 long-separation (~3.5cm) sources, 3 long-separation detectors (LD), and 3 short-separation (<1cm) detectors (SD) that covered PFC (4S, 1LD, 1SD), sensorimotor cortex (4S, 1LD, 1SD), and CER (4S, 1LD, 1SD). This long-separation optode montage was selected to match our low-channel count montage (Octamon+, Artinis Medical Systems, Netherlands) used in the stroke study where fNIRS sources were positioned at AF7, AF3, AF8, AF4, CP4, FC4, CP3, and FC3, and the two detectors were placed at the Cz and FPz with a source-detector distance of around 35mm (Rezaee et al., 2021). For CER fNIRS in this healthy human study, our fNIRS sources were positioned at the PO7, PO9, PO8, and PO10, and the detector was placed at Iz based on fNIRS Optodes' Location Decider (fOLD) (Zimeo Morais et al., 2018).

Data processing was conducted using open-source HOMER3 toolbox (Huppert et al., 2009) in Matlab (Mathworks Inc., USA). Raw optical intensity signal was first converted into optical density (function: hmrR_Intensity2OD), then motion artifact detection and correction was conducted using a hybrid method based on spline interpolation method and Savitzky–Golay filtering (function: hmrR_MotionCorrectSplineSG) (Jahani et al., 2018) using default parameters. Then, bandpass filtering was conducted (function:hmrR_BandpassFilt:Bandpass_Filter_OpticalDensity) within 0.01-0.1Hz followed by conversion to oxyhemoglobin (HbO) and deoxy-hemoglobin (HHb) concentration (function: hmrR_OD2Conc). Finally, hemodynamic response function (HRF) was computed using General Linear Model (GLM) (function: hmrR_GLM_new) with short separation regression performed with the nearest short separation channel. GLM determined the HRF during stimulation period from the

Preprints (www.preprints.org) | NOT PEER-REVIEWED | Posted: 4 January 2022 doi:10.20944/preprints202201.0008.v1

resting state using ordinary least squares (Ye et al., 2009) with consecutive sequence of Gaussian functions (stdev=0.5, step=0.5).

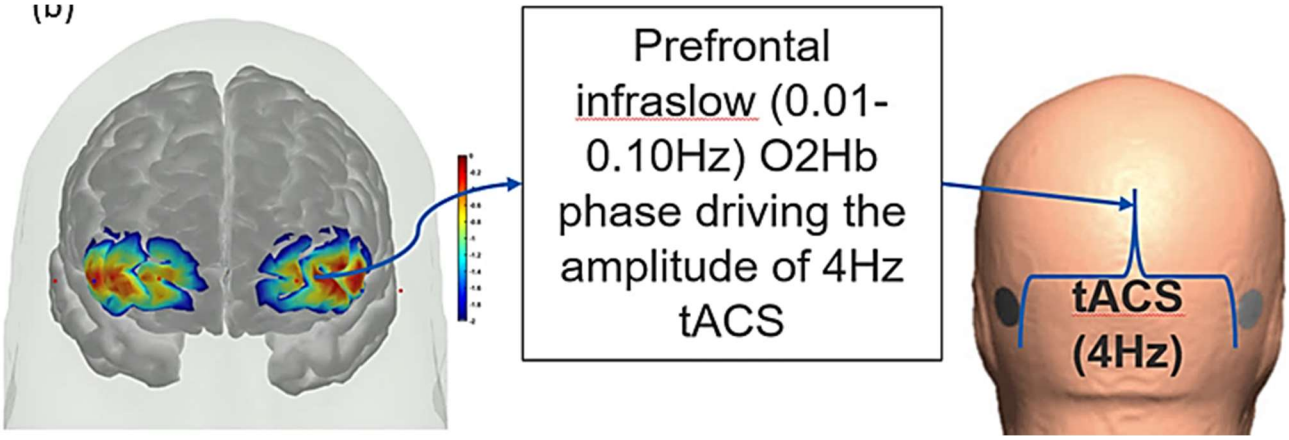

Figure 6: Illustration of PFC phase-amplitude coupled cerebellar tACS approach. Phase of the infraslow (0.01-0.10Hz) oxyhemoglobin (O2Hb) oscillations at the left lateral PFC driving the amplitude of the 4Hz cerebellar tACS optimized for targeting right lobules VI-CrusI/II-VIIb.

2.1.3 Optimization of electrode montage and fNIRS-driven ctACS

In prior work (Rezaee et al., 2021), we found a linear relationship between electric field distribution and the HbO response using GLM analysis of variance (ANOVA). In this study, we optimized the ctDCS/ctACS electrode montage for non-motor representation, i.e., right lobules VI-CrusI/II-VIIb, using EEG locations (Rezaee et al., 2020a). Amplitude of the 4Hz ctACS with optimized montage was driven by the phase of the infraslow (0.01-0.10Hz) HbO oscillations at left PFC found using Hilbert transform for the analytic signal using 60sec sliding window – see Figure 6. The maximum tACS amplitude was set at ±2 mA in the Starstim 8 tES device (Neuroelectrics).

3 Results

3.1 Computational modelling and simulation

3.1.1 Computational modelling of CBI

The left panel of Figure 7 shows the CBI recruitment curve at different intensities of the cerebellar TMS conditioning stimulus based on our prior work (Batsikadze et al., 2019). The conditioning TMS intensity was reduced in 5% steps below the brainstem motor threshold (BST) up to -25%. BST was determined by the corticospinal tract activation (shown in the left bottom brain section in Figure 3) by single-pulse TMS with the double-cone coil placed over the inion. The left panel of Figure 7 also shows the computed mean electric field (EF) at Crus II and DN, normalized by the maximum, at various conditioning TMS intensities (-5%, -10%, -15%, -20%, -25% BST). A “knee” was noticed around -15% BST when the CBI recruitment curve slope decreased (became flatter) for further increase in the conditioning TMS intensity – change point detection. This is postulated to be due to the stimulation of the DN (that is excitatory, shown by a blue marker in Figure 7) in addition to the Purkinje cells (that are inhibitory, shown by a red marker in Figure 7), resulting in a slower increase in CBI with increasing conditioning TMS intensity. The right panel shows the computed mean electric field (V/m) at Crus II and DN using CLOS, where the horizontal line denotes the DN mean electric field (V/m) at -15% BST, which is postulated to be the electric field (EF) threshold for DN activation. Here, all the mean EF (V/m) values at Crus II, which resulted in CBI (see left panel of Figure 7), were higher than the EF threshold for DN activation. Since motor evoked potential (MEP) cannot be generated at the non-motor

Preprints (www.preprints.org) | NOT PEER-REVIEWED | Posted: 4 January 2022 doi:10.20944/preprints202201.0008.v1

areas, so lobule-specific cerebellar NIBS (Batsikadze et al., 2019; Rezaee and Dutta, 2019, 2020; Rezaee et al., 2020a) can be combined with portable fNIRS-EEG joint-imaging to identify individual NIBS dose/response (also, non-responders) (Dutta et al., 2015; Guhathakurta and Dutta, 2016; Sood et al., 2016; Rezaee et al., 2020b).

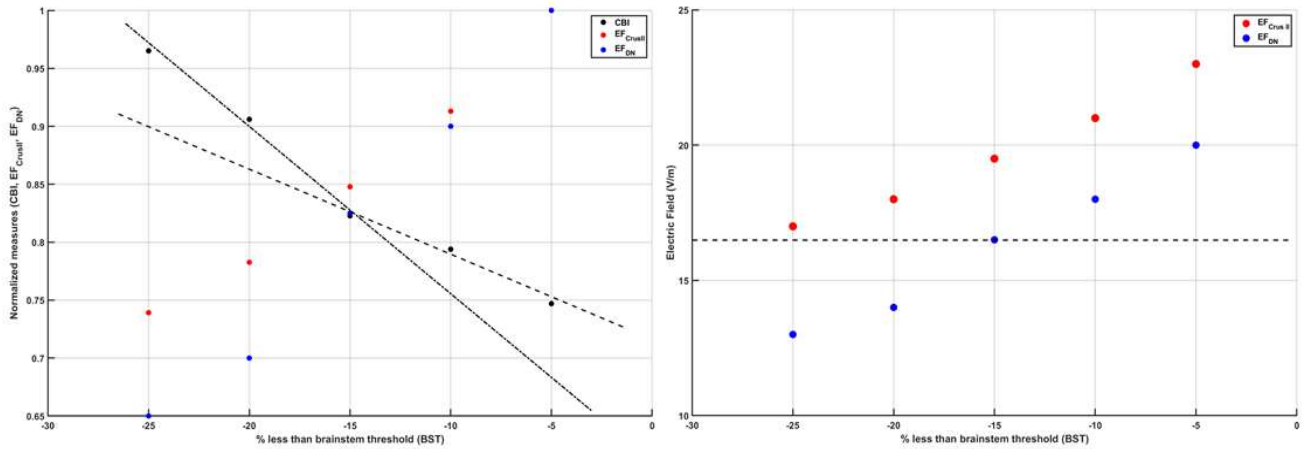

Figure 7: Left panel shows the change in the cerebellar brain inhibition (CBI) from a neurophysiological study and change in normalized (by maximum) electric field strength at Crus II and dentate nuclei (DN) with the change in the intensity of the transcranial magnetic stimulation (TMS) as a percent less than the brain stem threshold (BST). Right panel shows the electric field strength (V/m) at Crus II and dentate nuclei (DN) with the change in the intensity of the TMS as a percent less than the BST. -15% less that the BST is postulated to the TMS intensity (dash line in the right panel) at which DN starts getting activated by the TMS – change in the slope denoted by a dash and a dash-dot line in the left panel.

3.1.2 Computational modelling of ctDCS of inferior frontal gyrus and tTIS of DCN

Figure 8 shows our results from CLOS optimization for maximum electric field strength at the non-motor representation, right lobules VI-CrusI/II-VIIb (Rezaee and Dutta, 2019) based on a spatially unbiased atlas template (SUIT) of the human cerebellum (Diedrichsen, 2006) – see Figure 8a. Figure 8b shows that the optimized electric field strength in SUIT is focussed (>0.2151 V/m) at CrusI/II-VIIb lobules where 2mA at OI2 and -2mA at E145 were found optimal (see Figure 8c). Then, optimized cerebellar lobular and subsectional electric field strength showed that the deep nuclei received comparable electric field strength to cerebellar cortex (see Figure 8d). Then, Figure 8e shows the feasibility of fNIRS HbO based brain activation at the VLPFC including inferior frontal gyrus (Walia et al., 2021) that was targeted with 4x1 HD-tDCS as shown in Figure 8f, to facilitate post-retrieval control processes during VR-based extinction learning by amplifying downstream inhibition from the subthalamic nucleus for sensory gating (Kaji, 2001).

Preprints (www.preprints.org) | NOT PEER-REVIEWED | Posted: 4 January 2022 doi:10.20944/preprints202201.0008.v1

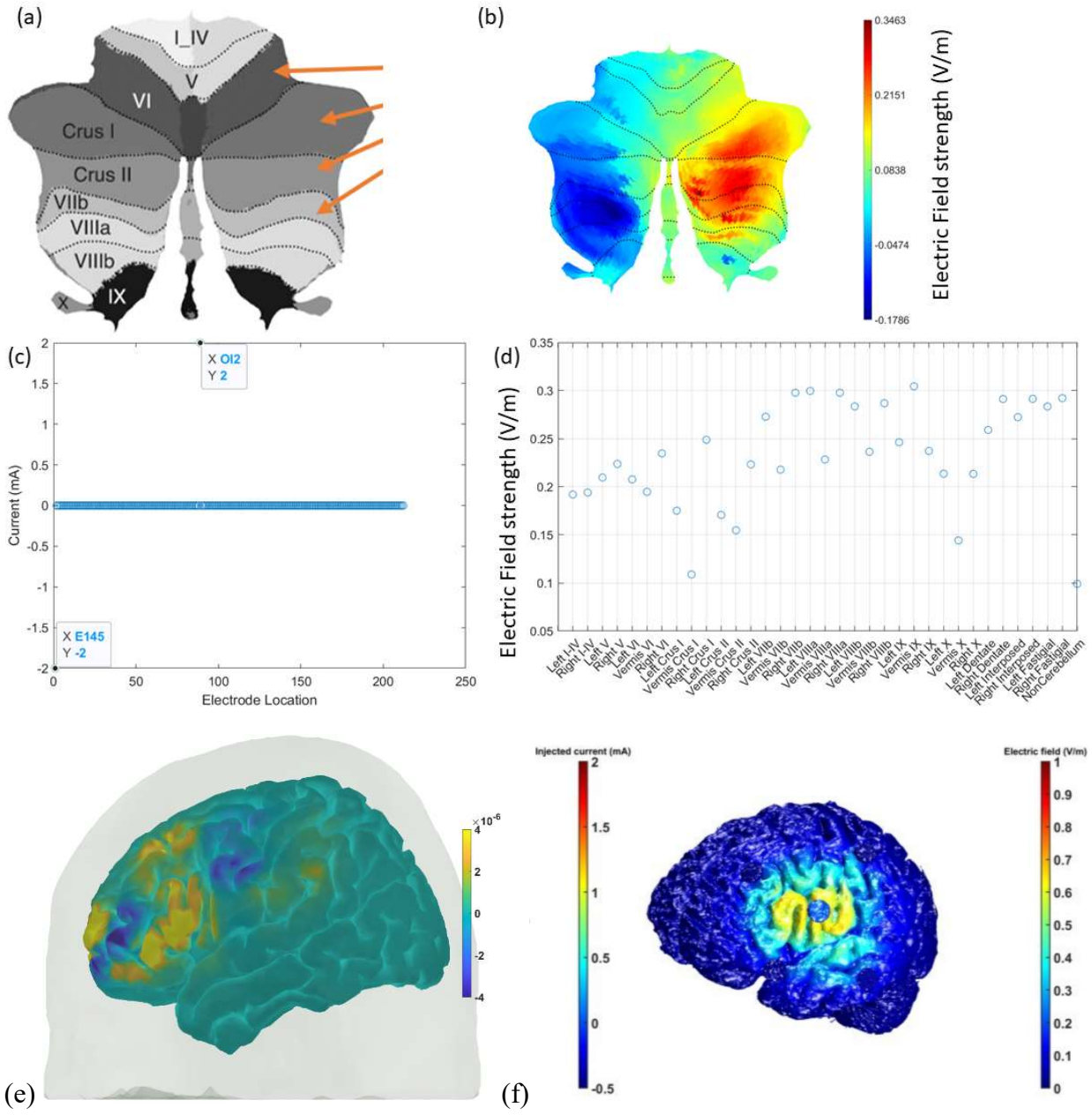

Figure 8: (a) A spatially unbiased atlas template (SUIT) of the human cerebellum and the ctDCS/ctACS targets shown with orange arrows for Cerebellar Lobules Optimal Stimulation (CLOS). (b) The electric field (V/m) strength in SUIT results from CLOS. (c) Electrode location results from CLOS for 2mA ctDCS/ctACS. (d) The cerebellar lobular and subsectional electric field (V/m) results from CLOS. (e) shows fNIRS HbO (in M) brain activation at the inferior frontal gyrus that can be targeted with HD-tDCS. (f) HD-tDCS montage to facilitate downstream inhibition from the subthalamic nucleus when substance-associated cues trigger substance-seeking.

Gamma-to-beta frequency shift can be considered a marker of sensory gating (Haenschel et al., 2000) that is postulated to be underpinned by cerebello-hippocampal interactions (Yu and Krook-Magnuson, 2015; Watson et al.). Cerebello-hippocampal connections have been found via the ventrolateral and laterodorsal thalamus in mice (Bohne et al., 2019) that needs further investigation in humans. However,

Preprints (www.preprints.org) | NOT PEER-REVIEWED | Posted: 4 January 2022 doi:10.20944/preprints202201.0008.v1

for our computational simulation based on a published model (Yousif et al., 2020), we postulated an effect of cerebellar tES on substance-seeking triggered by substance-associated cues since interactions between sensory and motor cortices can be modulated by the cerebellum (Lindeman et al., 2021). While ctDCS of the DCN induced gamma oscillations (top panel of Figure 9), bottom panel of the Figure 9 shows that tTIS of the DCN at 63Hz amplitude modulation could lead to gamma-to-beta frequency shift. Here, gamma frequency oscillations at the cortex can be generated with constant input (i.e., tDCS (Rezaee et al., 2020a),(Rezaee et al., 2021)) to the DCN while tTIS of DCN at 63Hz beats frequency (burst stimulation) led to beta frequency oscillations at the cortex (computational modelling details in the Supplementary Materials).

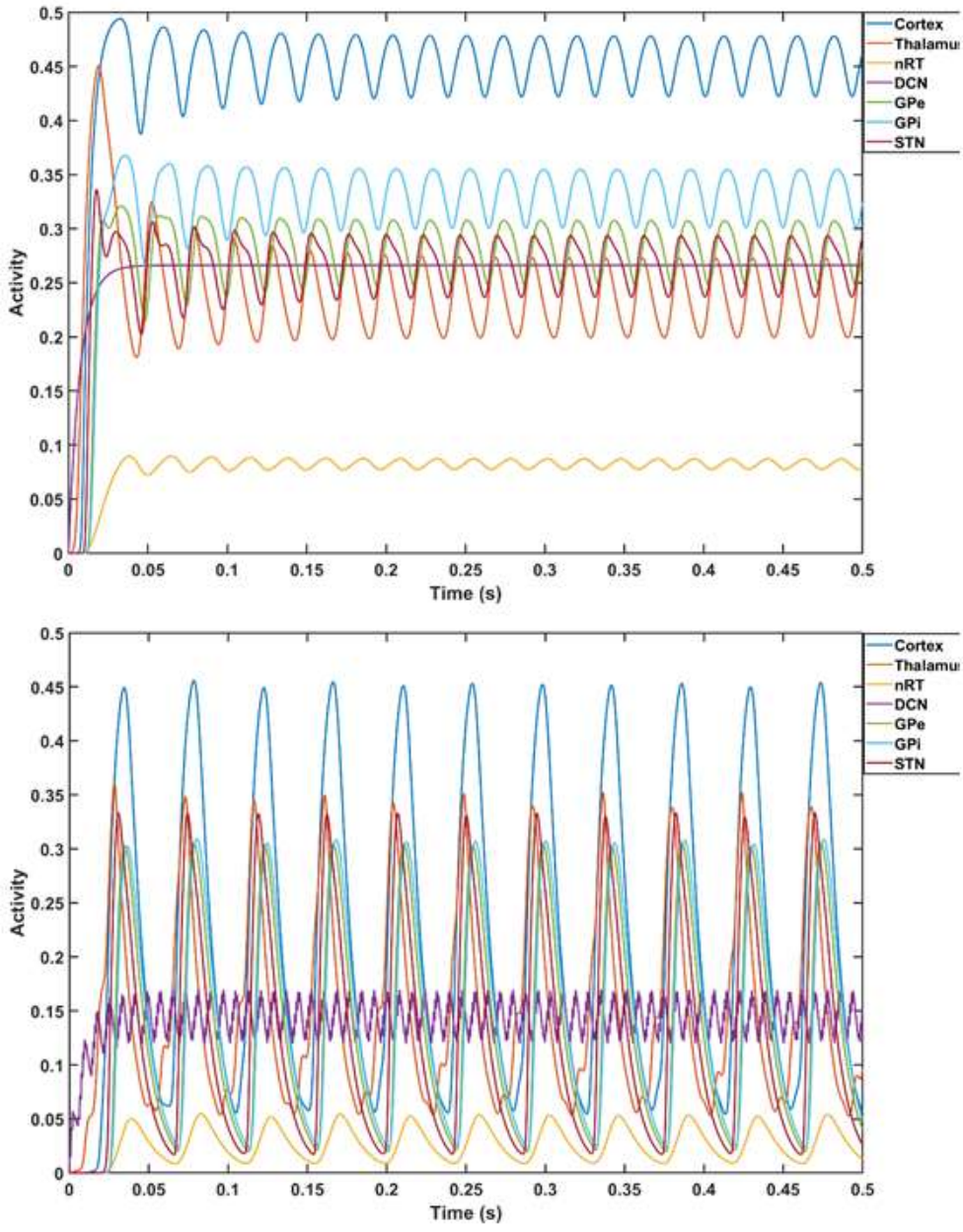

Figure 9: Computational modelling of thalamocortical basal ganglia with cerebellum (Yousif et al., 2020). Top panel shows the cortical gamma frequency oscillations with a constant external input to the dentate nucleus which transitions to beta frequency oscillations with tTIS of DN at 63Hz beats frequency.

Preprints (www.preprints.org) | NOT PEER-REVIEWED | Posted: 4 January 2022 doi:10.20944/preprints202201.0008.v1

3.2 fNIRS-driven cerebellar tES

3.2.1 fNIRS sensitivity profile

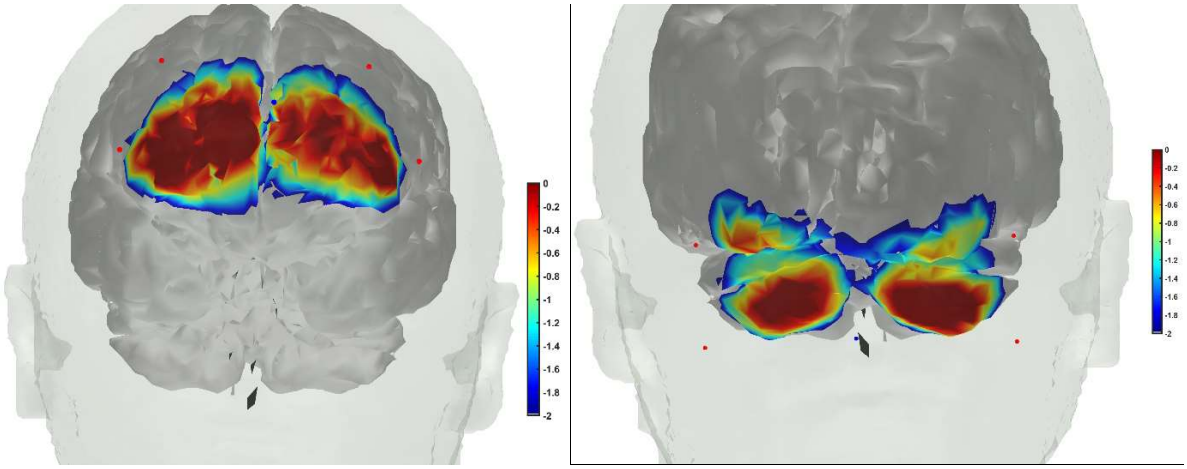

Figure 10: Left panel – fNIRS sensitivity profile where sources were positioned at AF7, AF3, AF8, AF4, and detector placed at the FPz. Right panel – fNIRS sensitivity profile where sources were positioned at PO7, PO9, PO8, and PO10, and the detector was placed at the Iz.

In this study, our PFC optode montage covered MPFC, and partly the DLPFC and VLPFC, as shown in the left panel of Figure 10. Right panel of Figure 10 shows the fNIRS sensitivity profile for CER optode montage (confirmed with fOLD (Zimeo Morais et al., 2018)) where we found from our MRI-based headmodel in AtlasViewer that the fNIRS sensitivity was mainly at the Crus I/II of the cerebellum. This is important since Crus I/II intersection is the intersection of first and the second default-mode representation (Guell and Schmahmann, 2020).

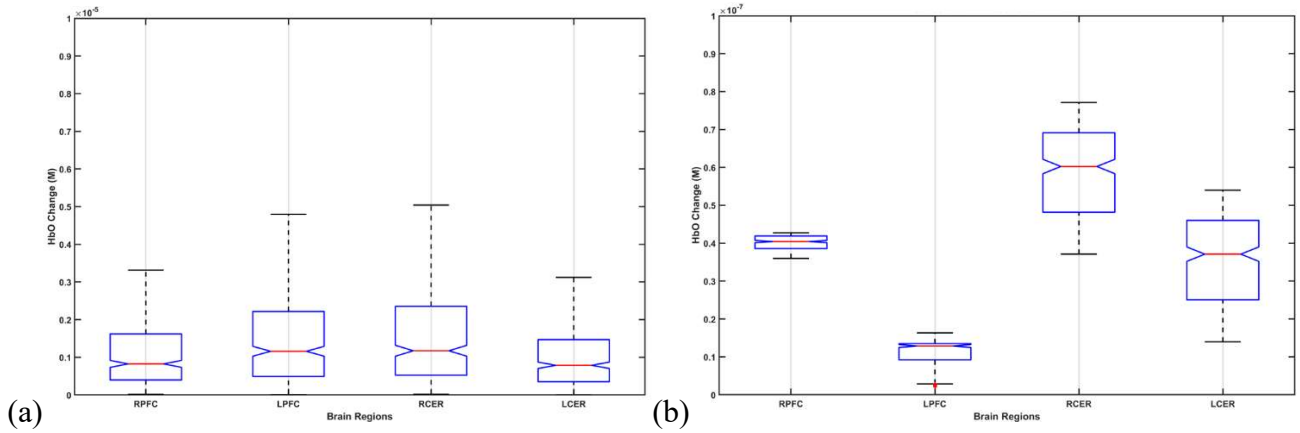

Figure 11: Box-plot of post-intervention HbO change from pre-intervention baseline due to 2mA ctDCS in (a) and ±2mA (max.) phase-amplitude-coupled ctACS in (b).

3.2.2 fNIRS HbO response to cerebellar tES

Computational modelling (Yousif et al., 2020) of the cerebrocerebellar connections of the afferent pathway (cerebello-thalamo-cortical) and the efferent pathway (cortico-ponto-cerebellar), as shown in Figure 1, is described in the Supplementary Materials. Here, the dysfunctional bidirectional interactions between DLPFC and the cerebellum can lead to dysrhythmia affecting sensory gating that may be ameliorated by cerebellar tES, as shown by simulation in Figure 9. Figure 11a shows the box-

Preprints (www.preprints.org) | NOT PEER-REVIEWED | Posted: 4 January 2022 doi:10.20944/preprints202201.0008.v1

plot of post-intervention HbO change where 2mA ctDCS evoked similar HbO change across brain regions (α=0.01). However, ±2mA (max.) phase-amplitude-coupled ctACS evoked HbO was lower but still statistically different (α=0.01) across those brain regions, as shown in Figure 11b. Moreover, increasing fNIRS-driven ctACS current to ±4mA increased HbO response in-the-range 10^{-6}M, which may affect the deep cerebellar nuclei (DCN) due to higher electric field strength. Therefore, tTIS need to be explored in future studies for specificity in targeting cerebellar cortex versus DCN – see Figure 1. The HbO responses are shown in the Supplementary Materials.

4 Discussion

This study presented a computational modelling and experimental methodological approach for portable neuroimaging guided NIBS, including cerebellar tTIS in CUD. NIBS intervention can be important at the early stages since CUD plays a causal role in the development of psychosis (Large et al., 2011) in certain genotypes with expression in cerebellum, as shown in Figure 2. The neurobiological substrate can be Δ(9)-tetrahydrocannabinol (THC), the main psychoactive constituent of cannabis, where chronic administration produced significant reductions in prepulse inhibition (PPI) that resemble that in schizophrenia (Tournier and Ginovart, 2014). However, cannabidiol in cannabis can have opposite effects on PPI (Saletti and Tomaz, 2019), which may be related to the antagonist of the human CB2 receptor (Kawamura et al., 2006; Thomas et al., 2007). Here, in cannabis use related psychotic disorders, we postulate a role of dysrhythmia of CCTC loop (as an extension of thalamocortical dysrhythmia (Schulman et al., 2011)) in sensorimotor gating including negative and positive symptoms due to dysfunction in the cerebellar cortex circuit. Here, we postulate that cerebellar NIBS may ameliorate the maladaptive plasticity as an adjuvant treatment to cue-reactivity training where cerebellar maladaptive plasticity may promote cannabis use related psychotic disorders in certain genotypes with expression in the cerebellum.

A key feature of psychotic disorders is the involvement of subcortical dopaminergic dysfunction (Kesby et al., 2018). Here, fundamental invasive neuroimaging studies in animal models can confirm the change of the cerebellar-brain connection using cerebellar TMS evoked dose response at the dopaminergic circuits based on multi-modal approach (Zachek et al., 2010; Park et al., 2011, 2012, 2013, 2017; Wickham et al., 2015) by incorporating extracellular electrophysiology and fast-scan cyclic voltammetry (FSCV) (Rodeberg et al., 2017) (tip diameter, ~1μm). Simultaneous multi-modal monitoring of (i) a local view (<100 μm) of rapid changes in dopamine (DA) concentration (≤10 ms), which will provide rTMS effects on VTA-DA regulation in MPFC and nucleus accumbens (NAc) subregions, and (ii) simultaneous electrophysiological data at the VTA, NAc, and MPFC over multiple spatial scales spanning individual neuronal spiking, population ensemble activity, and local field potential (LFP) oscillations (Lohani et al., 2019). However, TMS-based neuromodulation approaches are not amenable to home-based settings, so, tES should be investigated as an adjuvant treatment where cerebellar tDCS of Purkinje cells and DCN has been shown feasible (Rezaee et al., 2020a). Also, cerebellar tACS has been shown feasible in modulating motor behavior (Koganemaru et al., 2020); however, evidence for addiction medicine is limited (Ekhtiari et al., 2019). Recently, tES for deep brain stimulation has been shown feasible using temporally interfering electric fields (Grossman et al., 2017), so we presented a proof-of-concept computational simulation results in Figure 9. Also, NIBS of VLPFC including IFG (see Figure 8) can facilitate proactive control (Chambers et al., 2006; Leite et al., 2018) during cue-exposure therapy (Hone-Blanchet et al., 2014) which needs to be evaluated in clinical study. Based on our computational results, we presented experimental methodological approaches (Figure 4 and 5) for future experimental studies to investigate neuroimaging guided tES that can ameliorate CUD-related maladaptive plasticity and related dysfunctional cortical inhibition (Martin-Rodriguez et al., 2020). Furthermore, NIBS of the cerebellum in conjunction with the VLPFC including IFG is proposed

as an adjuvant treatment during early cue-exposure therapy may ameliorate chemical dependency as well as habit formation (Lewis, 2018).

In this study, we also performed feasibility testing of fNIRS of cerebellum and PFC. We found HbO response to ctDCS and ctACS using the same optimized montage (targeting right lobules VI-CrusI/II-VIIb). Specifically, we found 2mA ctDCS evoked similar (α=0.01) HbO responses across cerebellum and PFC brain regions that may be related to the modulation of Purkinje cells as well as deep cerebellar nuclei (see Figures 8d and 11) (Rezaee et al., 2020a). Indeed, tDCS can have effects on different cell populations that together will generate the effect which will be difficult to predict (Batsikadze et al., 2019) without grey-box modeling (Arora et al., 2021). Then, ctACS at the theta band frequency can increase the inhibitory tone that the cerebellum exerts over cerebrum due to postulated selective recruitment of cerebellar granule cells and Golgi cells (Spampinato et al., 2021). This modulation of the parallel fibre-Purkinje cell is postulated to lead to the modulation of the HbO activity at PFC that can then drive the ctACS via a phase amplitude coupling in our PFC phase-amplitude coupled ctACS approach – see Figure 7. Here, adequate lag in the phase amplitude coupling may be necessary that can be elucidated from HbO time series from the cerebellum and PFC – see Figure 10. In this preliminary study, we did not implement subject-specific lag for fNIRS-driven ctACS; however, we still found HbO change to be lower at the left PFC than the right PFC (see Figure 11b) during ctACS of the right lobules VI-CrusI/II-VIIb (HbO change higher in right than left cerebellum) indicating the recruitment of the cortico-cerebello-thalamo-cortical loop.

5 Conflict of Interest

The authors declare that the research was conducted in the absence of any commercial or financial relationships that could be construed as a potential conflict of interest.

6 Author Contributions

Conceptualization: Anirban Dutta.
Data curation: Pushpinder Walia.
Formal analysis: Pushpinder Walia, Anirban Dutta.
Funding acquisition: Anirban Dutta.
Investigation: Pushpinder Walia, Anirban Dutta.
Methodology: Pushpinder Walia, Anirban Dutta.
Software: Pushpinder Walia.
Writing – original draft: Anirban Dutta.
Writing – review & editing: Abhishek Ghosh, Shubhmohan Singh, Anirban Dutta.

7 Funding

Authors acknowledge the initial funding (2014−2017) by the Department of Science and Technology (DST), India and Institut National de Recherche en Informatique et en Automatique (Inria), France—https://team.inria.fr/nphys4nrehab/.

8 Acknowledgments

Authors would like to acknowledge the contributions from Dr. Uttama Lahiri at the Indian Institute of Technology, Gandhinagar, and Dr. MV Padma at the All India Institute Of Medical Sciences, New Delhi for the retrospective clinical data.

9 References

2019 NSDUH Detailed Tables | CBHSQ Data Available at: https://www.samhsa.gov/data/report/2019-nsduh-detailed-tables [Accessed October 18, 2020].

Aasted, C. M., Yücel, M. A., Cooper, R. J., Dubb, J., Tsuzuki, D., Becerra, L., et al. (2015a). Anatomical guidance for functional near-infrared spectroscopy: AtlasViewer tutorial. *Neurophotonics* 2, 020801. doi:10.1117/1.NPh.2.2.020801.

Aasted, C. M., Yücel, M. A., Cooper, R. J., Dubb, J., Tsuzuki, D., Becerra, L., et al. (2015b). Anatomical guidance for functional near-infrared spectroscopy: AtlasViewer tutorial. *Neurophotonics* 2. doi:10.1117/1.NPh.2.2.020801.

Administration (US), S. A. and M. H. S., and General (US), O. of the S. (2016). *THE NEUROBIOLOGY OF SUBSTANCE USE, MISUSE, AND ADDICTION*. US Department of Health and Human Services Available at: https://www.ncbi.nlm.nih.gov/books/NBK424849/ [Accessed March 15, 2021].

Alger, B. E., and Kim, J. (2011). Supply and demand for endocannabinoids. *Trends Neurosci* 34, 304–315. doi:10.1016/j.tins.2011.03.003.

Alves, P. N., Foulon, C., Karolis, V., Bzdok, D., Margulies, D. S., Volle, E., et al. (2019). An improved neuroanatomical model of the default-mode network reconciles previous neuroimaging and neuropathological findings. *Commun Biol* 2, 1–14. doi:10.1038/s42003-019-0611-3.

Aron, A. R., Robbins, T. W., and Poldrack, R. A. (2004). Inhibition and the right inferior frontal cortex. *Trends in Cognitive Sciences* 8, 170–177. doi:10.1016/j.tics.2004.02.010.

Arora, Y., Walia, P., Hayashibe, M., Muthalib, M., Chowdhury, S. R., Perrey, S., et al. (2021). Grey-box modeling and hypothesis testing of functional near-infrared spectroscopy-based cerebrovascular reactivity to anodal high-definition tDCS in healthy humans. doi:10.21203/rs.3.rs-83907/v3.

Badre, D., and Wagner, A. D. (2007). Left ventrolateral prefrontal cortex and the cognitive control of memory. *Neuropsychologia* 45, 2883–2901. doi:10.1016/j.neuropsychologia.2007.06.015.

Balleine, B. W., and O'Doherty, J. P. (2010). Human and Rodent Homologies in Action Control: Corticostriatal Determinants of Goal-Directed and Habitual Action. *Neuropsychopharmacology* 35, 48–69. doi:10.1038/npp.2009.131.

Barredo, J., Verstynen, T. D., and Badre, D. (2016). Organization of cortico-cortical pathways supporting memory retrieval across subregions of the left ventrolateral prefrontal cortex. *J Neurophysiol* 116, 920–937. doi:10.1152/jn.00157.2016.

Batsikadze, G., Rezaee, Z., Chang, D.-I., Gerwig, M., Herlitze, S., Dutta, A., et al. (2019). Effects of cerebellar transcranial direct current stimulation on cerebellar-brain inhibition in humans: A systematic evaluation. *Brain Stimulation: Basic, Translational, and Clinical Research in Neuromodulation* 0. doi:10.1016/j.brs.2019.04.010.

Bernard, J. A., and Mittal, V. A. (2014). Cerebellar-Motor Dysfunction in Schizophrenia and Psychosis-Risk: The Importance of Regional Cerebellar Analysis Approaches. *Front. Psychiatry* 5. doi:10.3389/fpsyt.2014.00160.

Bohne, P., Schwarz, M. K., Herlitze, S., and Mark, M. D. (2019). A New Projection From the Deep Cerebellar Nuclei to the Hippocampus via the Ventrolateral and Laterodorsal Thalamus in Mice. *Frontiers in Neural Circuits* 13, 51. doi:10.3389/fncir.2019.00051.

Brewer, J. R., Mazot, P., and Soriano, P. (2016). Genetic insights into the mechanisms of Fgf signaling. *Genes Dev.* 30, 751–771. doi:10.1101/gad.277137.115.

Brown, A. M., Arancillo, M., Lin, T., Catt, D. R., Zhou, J., Lackey, E. P., et al. (2019). Molecular layer interneurons shape the spike activity of cerebellar Purkinje cells. *Scientific Reports* 9, 1742. doi:10.1038/s41598-018-38264-1.

Buckner, R. L., Krienen, F. M., Castellanos, A., Diaz, J. C., and Yeo, B. T. T. (2011). The organization of the human cerebellum estimated by intrinsic functional connectivity. *J Neurophysiol* 106, 2322–2345. doi:10.1152/jn.00339.2011.

Carta, I., Chen, C. H., Schott, A. L., Dorizan, S., and Khodakhah, K. (2019). Cerebellar modulation of the reward circuitry and social behavior. *Science* 363. doi:10.1126/science.aav0581.

Carvalho, F., Brietzke, A. P., Gasparin, A., Dos Santos, F. P., Vercelino, R., Ballester, R. F., et al. (2018). Home-Based Transcranial Direct Current Stimulation Device Development: An Updated Protocol Used at Home in Healthy Subjects and Fibromyalgia Patients. *J Vis Exp*. doi:10.3791/57614.

Cerdá, M., Mauro, C., Hamilton, A., Levy, N. S., Santaella-Tenorio, J., Hasin, D., et al. (2020). Association Between Recreational Marijuana Legalization in the United States and Changes in Marijuana Use and Cannabis Use Disorder From 2008 to 2016. *JAMA Psychiatry* 77, 165–171. doi:10.1001/jamapsychiatry.2019.3254.

Chambers, C. D., Bellgrove, M. A., Stokes, M. G., Henderson, T. R., Garavan, H., Robertson, I. H., et al. (2006). Executive "brake failure" following deactivation of human frontal lobe. *J Cogn Neurosci* 18, 444–455. doi:10.1162/089892906775990606.

Claire Wilcox, M. D. (2019). A New Treatment for Substance Use Disorders? *NEJM Journal Watch* 2019. doi:10.1056/nejm-jw.NA49622.

Cousijn, J., Goudriaan, A. E., Ridderinkhof, K. R., Brink, W. van den, Veltman, D. J., and Wiers, R. W. (2013). Neural responses associated with cue-reactivity in frequent cannabis users. *Addiction Biology* 18, 570–580. doi:https://doi.org/10.1111/j.1369-1600.2011.00417.x.

Degenhardt, L., Charlson, F., Ferrari, A., Santomauro, D., Erskine, H., Mantilla-Herrara, A., et al. (2018). The global burden of disease attributable to alcohol and drug use in 195 countries and territories, 1990–2016: a systematic analysis for the Global Burden of Disease Study 2016. *The Lancet Psychiatry* 5, 987–1012. doi:10.1016/S2215-0366(18)30337-7.

Degenhardt, L., Ferrari, A. J., Calabria, B., Hall, W. D., Norman, R. E., McGrath, J., et al. (2013). The global epidemiology and contribution of cannabis use and dependence to the global

burden of disease: results from the GBD 2010 study. *PLoS One* 8, e76635. doi:10.1371/journal.pone.0076635.

Di Forti, M., Iyegbe, C., Sallis, H., Kolliakou, A., Falcone, M. A., Paparelli, A., et al. (2012). Confirmation that the AKT1 (rs2494732) genotype influences the risk of psychosis in cannabis users. *Biol Psychiatry* 72, 811–816. doi:10.1016/j.biopsych.2012.06.020.

Di Marzo, V., Stella, N., and Zimmer, A. (2015). Endocannabinoid signalling and the deteriorating brain. *Nat Rev Neurosci* 16, 30–42. doi:10.1038/nrn3876.

Diedrichsen, J. (2006). A spatially unbiased atlas template of the human cerebellum. *Neuroimage* 33, 127–138. doi:10.1016/j.neuroimage.2006.05.056.

Dorgans, K., Demais, V., Bailly, Y., Poulain, B., Isope, P., and Doussau, F. (2019). Short-term plasticity at cerebellar granule cell to molecular layer interneuron synapses expands information processing. *eLife* 8, e41586. doi:10.7554/eLife.41586.

Dutta, A., Jacob, A., Chowdhury, S. R., Das, A., and Nitsche, M. A. (2015). EEG-NIRS based assessment of neurovascular coupling during anodal transcranial direct current stimulation--a stroke case series. *J Med Syst* 39, 205. doi:10.1007/s10916-015-0205-7.

Dutta, A., Karanth, S. S., Bhattacharya, M., Liput, M., Augustyniak, J., Cheung, M., et al. (2020). A proof of concept 'phase zero' study of neurodevelopment using brain organoid models with Vis/near-infrared spectroscopy and electrophysiology. *Scientific Reports* 10, 20987. doi:10.1038/s41598-020-77929-8.

Ekhtiari, H., Tavakoli, H., Addolorato, G., Baeken, C., Bonci, A., Campanella, S., et al. (2019). Transcranial electrical and magnetic stimulation (tES and TMS) for addiction medicine: A consensus paper on the present state of the science and the road ahead. *Neurosci Biobehav Rev* 104, 118–140. doi:10.1016/j.neubiorev.2019.06.007.

Fernandez, L., Rogasch, N. C., Do, M., Clark, G., Major, B. P., Teo, W.-P., et al. (2020). Cerebral Cortical Activity Following Non-invasive Cerebellar Stimulation—a Systematic Review of Combined TMS and EEG Studies. *Cerebellum* 19, 309–335. doi:10.1007/s12311-019-01093-7.

Gao, R., and Penzes, P. (2015). Common Mechanisms of Excitatory and Inhibitory Imbalance in Schizophrenia and Autism Spectrum Disorders. *Curr Mol Med* 15, 146–167.

Goldstein, R. Z., and Volkow, N. D. (2011). Dysfunction of the prefrontal cortex in addiction: neuroimaging findings and clinical implications. *Nat Rev Neurosci* 12, 652–669. doi:10.1038/nrn3119.

Grossman, N., Bono, D., Dedic, N., Kodandaramaiah, S. B., Rudenko, A., Suk, H.-J., et al. (2017). Noninvasive Deep Brain Stimulation via Temporally Interfering Electric Fields. *Cell* 169, 1029-1041.e16. doi:10.1016/j.cell.2017.05.024.

Guell, X., and Schmahmann, J. (2020). Cerebellar Functional Anatomy: a Didactic Summary Based on Human fMRI Evidence. *Cerebellum* 19, 1–5. doi:10.1007/s12311-019-01083-9.

Guhathakurta, D., and Dutta, A. (2016). Computational Pipeline for NIRS-EEG Joint Imaging of tDCS-Evoked Cerebral Responses—An Application in Ischemic Stroke. *Front. Neurosci.* 10. doi:10.3389/fnins.2016.00261.

Haenschel, C., Baldeweg, T., Croft, R. J., Whittington, M., and Gruzelier, J. (2000). Gamma and beta frequency oscillations in response to novel auditory stimuli: A comparison of human electroencephalogram (EEG) data with in vitro models. *PNAS* 97, 7645–7650. doi:10.1073/pnas.120162397.

Haluk, D. M., and Floresco, S. B. (2009). Ventral striatal dopamine modulation of different forms of behavioral flexibility. *Neuropsychopharmacology* 34, 2041–2052. doi:10.1038/npp.2009.21.

Hanlon, C. A., Dowdle, L. T., and Henderson, J. S. (2018). Modulating Neural Circuits with Transcranial Magnetic Stimulation: Implications for Addiction Treatment Development. *Pharmacol Rev* 70, 661–683. doi:10.1124/pr.116.013649.

Hirano, T. (2013). "GABA and Synaptic Transmission in the Cerebellum," in *Handbook of the Cerebellum and Cerebellar Disorders*, eds. M. Manto, J. D. Schmahmann, F. Rossi, D. L. Gruol, and N. Koibuchi (Dordrecht: Springer Netherlands), 881–893. doi:10.1007/978-94-007-1333-8_36.

Hirvonen, J., Goodwin, R. S., Li, C.-T., Terry, G. E., Zoghbi, S. S., Morse, C., et al. (2012). Reversible and regionally selective downregulation of brain cannabinoid CB 1 receptors in chronic daily cannabis smokers. *Molecular Psychiatry* 17, 642–649. doi:10.1038/mp.2011.82.

Hone-Blanchet, A., Wensing, T., and Fecteau, S. (2014). The Use of Virtual Reality in Craving Assessment and Cue-Exposure Therapy in Substance Use Disorders. *Front. Hum. Neurosci.* 8. doi:10.3389/fnhum.2014.00844.

Hong, L. E., Summerfelt, A., McMahon, R. P., Thaker, G. K., and Buchanan, R. W. (2004). Gamma/beta oscillation and sensory gating deficit in schizophrenia. *Neuroreport* 15, 155–159. doi:10.1097/00001756-200401190-00030.

Hu, C., Zhang, L.-B., Chen, H., Xiong, Y., and Hu, B. (2015). Neurosubstrates and mechanisms underlying the extinction of associative motor memory. *Neurobiology of Learning and Memory* 126, 78–86. doi:10.1016/j.nlm.2015.07.009.

Huang, Y., Datta, A., Bikson, M., and Parra, L. C. (2019). Realistic volumetric-approach to simulate transcranial electric stimulation—ROAST—a fully automated open-source pipeline. *J. Neural Eng.* 16, 056006. doi:10.1088/1741-2552/ab208d.

Huang, Y., Liu, A. A., Lafon, B., Friedman, D., Dayan, M., Wang, X., et al. (2017). Measurements and models of electric fields in the in vivo human brain during transcranial electric stimulation. *eLife* 6. doi:10.7554/eLife.18834.

Huhn, A. S., Sweeney, M. M., Brooner, R. K., Kidorf, M. S., Tompkins, D. A., Ayaz, H., et al. (2019). Prefrontal cortex response to drug cues, craving, and current depressive symptoms are associated with treatment outcomes in methadone-maintained patients. *Neuropsychopharmacology* 44, 826–833. doi:10.1038/s41386-018-0252-0.

Huppert, T. J., Diamond, S. G., Franceschini, M. A., and Boas, D. A. (2009). HomER: a review of time-series analysis methods for near-infrared spectroscopy of the brain. *Appl Opt* 48, D280–D298.

Ishikawa, T., Tomatsu, S., Tsunoda, Y., Lee, J., Hoffman, D. S., and Kakei, S. (2014). Releasing dentate nucleus cells from Purkinje cell inhibition generates output from the cerebrocerebellum. *PLoS ONE* 9, e108774. doi:10.1371/journal.pone.0108774.

Jahani, S., Setarehdan, S. K., Boas, D. A., and Yücel, M. A. (2018). Motion artifact detection and correction in functional near-infrared spectroscopy: a new hybrid method based on spline interpolation method and Savitzky–Golay filtering. *Neurophotonics* 5. doi:10.1117/1.NPh.5.1.015003.

Johnson, L., Alekseichuk, I., Krieg, J., Doyle, A., Yu, Y., Vitek, J., et al. (2020). Dose-dependent effects of transcranial alternating current stimulation on spike timing in awake nonhuman primates. *Science Advances* 6, eaaz2747. doi:10.1126/sciadv.aaz2747.

Kaji, R. (2001). Basal ganglia as a sensory gating devise for motor control. *J Med Invest* 48, 142–146.

Kawamura, Y., Fukaya, M., Maejima, T., Yoshida, T., Miura, E., Watanabe, M., et al. (2006). The CB1 cannabinoid receptor is the major cannabinoid receptor at excitatory presynaptic sites in the hippocampus and cerebellum. *J Neurosci* 26, 2991–3001. doi:10.1523/JNEUROSCI.4872-05.2006.

Kedzior, K. K., and Martin-Iverson, M. T. (2006). Chronic cannabis use is associated with attention-modulated reduction in prepulse inhibition of the startle reflex in healthy humans. *J Psychopharmacol* 20, 471–484. doi:10.1177/0269881105057516.

Kendler, K. S., Lönn, S. L., Sundquist, J., and Sundquist, K. (2015). Smoking and schizophrenia in population cohorts of Swedish women and men: a prospective co-relative control study. *Am J Psychiatry* 172, 1092–1100. doi:10.1176/appi.ajp.2015.15010126.

Kesby, J. P., Eyles, D. W., McGrath, J. J., and Scott, J. G. (2018). Dopamine, psychosis and schizophrenia: the widening gap between basic and clinical neuroscience. *Translational Psychiatry* 8, 1–12. doi:10.1038/s41398-017-0071-9.

Kimpel, O., Hulst, T., Batsikadze, G., Ernst, T. M., Nitsche, M. A., Timmann, D., et al. (2020). Long-term effects of cerebellar anodal transcranial direct current stimulation (tDCS) on the acquisition and extinction of conditioned eyeblink responses. *Scientific Reports* 10, 22434. doi:10.1038/s41598-020-80023-8.

Klejbor, I., Kucinski, A., Wersinger, S. R., Corso, T., Spodnik, J. H., Dziewiatkowski, J., et al. (2009). Serotonergic hyperinnervation and effective serotonin blockade in an FGF receptor developmental model of psychosis. *Schizophr Res* 113, 308–321. doi:10.1016/j.schres.2009.06.006.

Koffarnus, M. N., Jarmolowicz, D. P., Mueller, E. T., and Bickel, W. K. (2013). Changing Delay Discounting in the Light of the Competing Neurobehavioral Decision Systems Theory: a Review. *J Exp Anal Behav* 99, 32–57. doi:10.1002/jeab.2.

Koganemaru, S., Mikami, Y., Matsuhashi, M., Truong, D. Q., Bikson, M., Kansaku, K., et al. (2020). Cerebellar transcranial alternating current stimulation modulates human gait rhythm. *Neurosci Res* 156, 265–270. doi:10.1016/j.neures.2019.12.003.

Krienen, F. M., and Buckner, R. L. (2009). Segregated fronto-cerebellar circuits revealed by intrinsic functional connectivity. *Cereb. Cortex* 19, 2485–2497. doi:10.1093/cercor/bhp135.

Kuepper, R., van Os, J., Lieb, R., Wittchen, H.-U., Höfler, M., and Henquet, C. (2011). Continued cannabis use and risk of incidence and persistence of psychotic symptoms: 10 year follow-up cohort study. *BMJ* 342, d738. doi:10.1136/bmj.d738.

Kumar, D., Dutta, A., Das, A., and Lahiri, U. (2016). SmartEye: Developing a Novel Eye Tracking System for Quantitative Assessment of Oculomotor Abnormalities. *IEEE Trans Neural Syst Rehabil Eng* 24, 1051–1059. doi:10.1109/TNSRE.2016.2518222.

Large, M., Sharma, S., Compton, M. T., Slade, T., and Nielssen, O. (2011). Cannabis use and earlier onset of psychosis: a systematic meta-analysis. *Arch Gen Psychiatry* 68, 555–561. doi:10.1001/archgenpsychiatry.2011.5.

Lee, S., Lee, C., Park, J., and Im, C.-H. (2020). Individually customized transcranial temporal interference stimulation for focused modulation of deep brain structures: a simulation study with different head models. *Scientific Reports* 10, 11730. doi:10.1038/s41598-020-68660-5.

Leite, J., Gonçalves, Ó. F., Pereira, P., Khadka, N., Bikson, M., Fregni, F., et al. (2018). The differential effects of unihemispheric and bihemispheric tDCS over the inferior frontal gyrus on proactive control. *Neurosci Res* 130, 39–46. doi:10.1016/j.neures.2017.08.005.

Levy, B. J., and Wagner, A. D. (2011). Cognitive control and right ventrolateral prefrontal cortex: reflexive reorienting, motor inhibition, and action updating. *Ann N Y Acad Sci* 1224, 40–62. doi:10.1111/j.1749-6632.2011.05958.x.

Lewis, M. (2018). Brain Change in Addiction as Learning, Not Disease. *N Engl J Med* 379, 1551–1560. doi:10.1056/NEJMra1602872.

Lindeman, S., Hong, S., Kros, L., Mejias, J. F., Romano, V., Oostenveld, R., et al. (2021). Cerebellar Purkinje cells can differentially modulate coherence between sensory and motor cortex depending on region and behavior. *PNAS* 118. doi:10.1073/pnas.2015292118.

Lohani, S., Martig, A. K., Deisseroth, K., Witten, I. B., and Moghaddam, B. (2019). Dopamine Modulation of Prefrontal Cortex Activity Is Manifold and Operates at Multiple Temporal and Spatial Scales. *Cell Reports* 27, 99-114.e6. doi:10.1016/j.celrep.2019.03.012.

Macleod, J., Oakes, R., Copello, A., Crome, I., Egger, M., Hickman, M., et al. (2004). Psychological and social sequelae of cannabis and other illicit drug use by young people: a systematic review of longitudinal, general population studies. *Lancet* 363, 1579–1588. doi:10.1016/S0140-6736(04)16200-4.

Makani, R., Pradhan, B., Shah, U., and Parikh, T. (2017). Role of Repetitive Transcranial Magnetic Stimulation (rTMS) in Treatment of Addiction and Related Disorders: A Systematic Review. *Curr Drug Abuse Rev* 10, 31–43. doi:10.2174/1874473710666171129225914.

Mannarelli, D., Pauletti, C., Currà, A., Marinelli, L., Corrado, A., Delle Chiaie, R., et al. (2019). The Cerebellum Modulates Attention Network Functioning: Evidence from a Cerebellar Transcranial Direct Current Stimulation and Attention Network Test Study. *Cerebellum* 18, 457–468. doi:10.1007/s12311-019-01014-8.

Mannarelli, D., Pauletti, C., Petritis, A., Delle Chiaie, R., Currà, A., Trompetto, C., et al. (2020). Effects of Cerebellar tDCS on Inhibitory Control: Evidence from a Go/NoGo Task. *Cerebellum* 19, 788–798. doi:10.1007/s12311-020-01165-z.

Marcaggi, P. (2015). Cerebellar endocannabinoids: retrograde signaling from purkinje cells. *Cerebellum* 14, 341–353. doi:10.1007/s12311-014-0629-5.

Marek, S., Siegel, J. S., Gordon, E. M., Raut, R. V., Gratton, C., Newbold, D. J., et al. (2018). Spatial and Temporal Organization of the Individual Human Cerebellum. *Neuron* 100, 977-993.e7. doi:10.1016/j.neuron.2018.10.010.

Martin-Rodriguez, J. F., Ruiz-Veguilla, M., Alvarez de Toledo, P., Aizpurua-Olaizola, O., Zarandona, I., Canal-Rivero, M., et al. (2020). Impaired motor cortical plasticity associated with cannabis use disorder in young adults. *Addict Biol*, e12912. doi:10.1111/adb.12912.

Middleton, F. A., and Strick, P. L. (2001). Cerebellar Projections to the Prefrontal Cortex of the Primate. *J. Neurosci.* 21, 700–712. doi:10.1523/JNEUROSCI.21-02-00700.2001.

Mikkonen, M., Laakso, I., Tanaka, S., and Hirata, A. (2020). Cost of focality in TDCS: Interindividual variability in electric fields. *Brain Stimulation* 13, 117–124. doi:10.1016/j.brs.2019.09.017.

Morellini, N., Grehl, S., Tang, A., Rodger, J., Mariani, J., Lohof, A. M., et al. (2015). What does low-intensity rTMS do to the cerebellum? *Cerebellum* 14, 23–26. doi:10.1007/s12311-014-0617-9.

Moulton, E. A., Elman, I., Becerra, L. R., Goldstein, R. Z., and Borsook, D. (2014). The Cerebellum and Addiction: Insights Gained from Neuroimaging Research. *Addict Biol* 19, 317–331.

Myers, K. M., and Carlezon Jr., W. A. (2010). Extinction of drug- and withdrawal-paired cues in animal models: Relevance to the treatment of addiction. *Neuroscience and Biobehavioral Reviews* 35, 285–302. doi:10.1016/j.neubiorev.2010.01.011.

Nitsche, M. A., and Paulus, W. (2001). Sustained excitability elevations induced by transcranial DC motor cortex stimulation in humans. *Neurology* 57, 1899–1901. doi:10.1212/wnl.57.10.1899.

Page, C. E., and Coutellier, L. (2018). Reducing inhibition: A promising new strategy for the treatment of schizophrenia. *EBioMedicine* 35, 25–26. doi:10.1016/j.ebiom.2018.07.043.

Paquette, C., Sidel, M., Radinska, B. A., Soucy, J.-P., and Thiel, A. (2011). Bilateral transcranial direct current stimulation modulates activation-induced regional blood flow changes during voluntary movement. *J Cereb Blood Flow Metab* 31, 2086–2095. doi:10.1038/jcbfm.2011.72.

Park, J., Bucher, E. S., Fontillas, K., Owesson-White, C., Ariansen, J. L., Carelli, R. M., et al. (2013). Opposing Catecholamine Changes in the Bed Nucleus of the Stria Terminalis during

Intracranial Self-Stimulation and its Extinction. *Biol Psychiatry* 74, 69–76. doi:10.1016/j.biopsych.2012.11.008.

Park, J., Takmakov, P., and Wightman, R. M. (2011). In Vivo Comparison of Norepinephrine and Dopamine Release in Rat Brain by Simultaneous Measurements with Fast-Scan Cyclic Voltammetry. *J Neurochem* 119, 932–944. doi:10.1111/j.1471-4159.2011.07494.x.

Park, J. W., Bhimani, R. V., and Park, J. (2017). Noradrenergic Modulation of Dopamine Transmission Evoked by Electrical Stimulation of the Locus Coeruleus in the Rat Brain. *ACS Chem. Neurosci.* 8, 1913–1924. doi:10.1021/acschemneuro.7b00078.

Park, J., Wheeler, R. A., Fontillas, K., Keithley, R. B., Carelli, R. M., and Wightman, R. M. (2012). Catecholamines in the Bed Nucleus of the Stria Terminalis Reciprocally Respond to Reward and Aversion. *Biol Psychiatry* 71, 327–334. doi:10.1016/j.biopsych.2011.10.017.

Pinti, P., Merla, A., Aichelburg, C., Lind, F., Power, S., Swingler, E., et al. (2017). A novel GLM-based method for the Automatic IDentification of functional Events (AIDE) in fNIRS data recorded in naturalistic environments. *Neuroimage* 155, 291–304. doi:10.1016/j.neuroimage.2017.05.001.

Power, R. A., Verweij, K. J. H., Zuhair, M., Montgomery, G. W., Henders, A. K., Heath, A. C., et al. (2014). Genetic predisposition to schizophrenia associated with increased use of cannabis. *Mol Psychiatry* 19, 1201–1204. doi:10.1038/mp.2014.51.

Pripfl, J., Tomova, L., Riecansky, I., and Lamm, C. (2014). Transcranial magnetic stimulation of the left dorsolateral prefrontal cortex decreases cue-induced nicotine craving and EEG delta power. *Brain Stimul* 7, 226–233. doi:10.1016/j.brs.2013.11.003.

Rae, C. L., Hughes, L. E., Anderson, M. C., and Rowe, J. B. (2015). The Prefrontal Cortex Achieves Inhibitory Control by Facilitating Subcortical Motor Pathway Connectivity. *J Neurosci* 35, 786–794. doi:10.1523/JNEUROSCI.3093-13.2015.

Rampersad, S. M., Janssen, A. M., Lucka, F., Aydin, Ü., Lanfer, B., Lew, S., et al. (2014). Simulating transcranial direct current stimulation with a detailed anisotropic human head model. *IEEE Trans Neural Syst Rehabil Eng* 22, 441–452. doi:10.1109/TNSRE.2014.2308997.

Rezaee, Z., and Dutta, A. (2019). A computational pipeline to optimize lobule-specific electric field distribution during cerebellar transcranial direct current stimulation. *Front. Neurosci.* 13. doi:10.3389/fnins.2019.00266.

Rezaee, Z., and Dutta, A. (2020). Lobule-Specific Dosage Considerations for Cerebellar Transcranial Direct Current Stimulation During Healthy Aging: A Computational Modeling Study Using Age-Specific Magnetic Resonance Imaging Templates. *Neuromodulation*. doi:10.1111/ner.13098.

Rezaee, Z., Kaura, S., Solanki, D., Dash, A., Srivastava, M. V. P., Lahiri, U., et al. (2020a). Deep Cerebellar Transcranial Direct Current Stimulation of the Dentate Nucleus to Facilitate Standing Balance in Chronic Stroke Survivors—A Pilot Study. *Brain Sciences* 10, 94. doi:10.3390/brainsci10020094.

Rezaee, Z., Ranjan, S., Solanki, D., Bhattacharya, M., Srivastava, M. P., Lahiri, U., et al. (2020b). Functional near-infrared spectroscopy in conjunction with electroencephalography of cerebellar transcranial direct current stimulation responses in the latent neurovascular coupling space – a chronic stroke study. *bioRxiv*, 2020.05.24.113928. doi:10.1101/2020.05.24.113928.

Rezaee, Z., Ranjan, S., Solanki, D., Bhattacharya, M., Srivastava, M. V. P., Lahiri, U., et al. (2021). Feasibility of combining functional near-infrared spectroscopy with electroencephalography to identify chronic stroke responders to cerebellar transcranial direct current stimulation-a computational modeling and portable neuroimaging methodological study. *Cerebellum*. doi:10.1007/s12311-021-01249-4.

Rodeberg, N. T., Sandberg, S. G., Johnson, J. A., Phillips, P. E. M., and Wightman, R. M. (2017). Hitchhiker's Guide to Voltammetry: Acute and Chronic Electrodes for in Vivo Fast-Scan Cyclic Voltammetry. *ACS Chem. Neurosci.* 8, 221–234. doi:10.1021/acschemneuro.6b00393.

ROGERS, T. D., DICKSON, P. E., HECK, D. H., GOLDOWITZ, D., MITTLEMAN, G., and BLAHA, C. D. (2011). Connecting the Dots of the Cerebro-Cerebellar Role in Cognitive Function: Neuronal Pathways for Cerebellar Modulation of Dopamine Release in the Prefrontal Cortex. *Synapse* 65. doi:10.1002/syn.20960.

Rohleder, C., Wiedermann, D., Neumaier, B., Drzezga, A., Timmermann, L., Graf, R., et al. (2016). The Functional Networks of Prepulse Inhibition: Neuronal Connectivity Analysis Based on FDG-PET in Awake and Unrestrained Rats. *Front Behav Neurosci* 10. doi:10.3389/fnbeh.2016.00148.

Sadanandan, S. M., Kreko-Pierce, T., Khatri, S. N., and Pugh, J. R. (2020). Cannabinoid type 2 receptors inhibit GABAA receptor-mediated currents in cerebellar Purkinje cells of juvenile mice. *PLOS ONE* 15, e0233020. doi:10.1371/journal.pone.0233020.

Sahlem, G. L., Baker, N. L., George, M. S., Malcolm, R. J., and McRae-Clark, A. L. (2018). Repetitive transcranial magnetic stimulation (rTMS) administration to heavy cannabis users. *Am J Drug Alcohol Abuse* 44, 47–55. doi:10.1080/00952990.2017.1355920.

Saletti, P. G., and Tomaz, C. (2019). Cannabidiol effects on prepulse inhibition in nonhuman primates. *Reviews in the Neurosciences* 30, 95–105. doi:10.1515/revneuro-2017-0101.

Saturnino, G. B., Puonti, O., Nielsen, J. D., Antonenko, D., Madsen, K. H. H., and Thielscher, A. (2018). SimNIBS 2.1: A Comprehensive Pipeline for Individualized Electric Field Modelling for Transcranial Brain Stimulation. *bioRxiv*, 500314. doi:10.1101/500314.

Schacht, J. P., Anton, R. F., and Myrick, H. (2013). Functional neuroimaging studies of alcohol cue reactivity: a quantitative meta-analysis and systematic review. *Addict Biol* 18, 121–133. doi:10.1111/j.1369-1600.2012.00464.x.

Schulman, J. J., Cancro, R., Lowe, S. I., Lu, F., Walton, K. D., and Llinás, R. R. (2011). Imaging of Thalamocortical Dysrhythmia in Neuropsychiatry. *Front. Hum. Neurosci.* 5. doi:10.3389/fnhum.2011.00069.

Shumay, E., Wiers, C. E., Shokri-Kojori, E., Kim, S. W., Hodgkinson, C. A., Sun, H., et al. (2017). New Repeat Polymorphism in the AKT1 Gene Predicts Striatal Dopamine D2/D3 Receptor Availability and Stimulant-Induced Dopamine Release in the Healthy Human Brain. *J. Neurosci.* 37, 4982–4991. doi:10.1523/JNEUROSCI.3155-16.2017.

Sood, M., Besson, P., Muthalib, M., Jindal, U., Perrey, S., Dutta, A., et al. (2016). NIRS-EEG joint imaging during transcranial direct current stimulation: Online parameter estimation with an autoregressive model. *J. Neurosci. Methods* 274, 71–80. doi:10.1016/j.jneumeth.2016.09.008.

Spampinato, D., Avci, E., Rothwell, J., and Rocchi, L. (2021). Frequency-dependent modulation of cerebellar excitability during the application of non-invasive alternating current stimulation. *Brain Stimul* 14, 277–283. doi:10.1016/j.brs.2021.01.007.

Stein, E. R., Gibson, B. C., Votaw, V. R., Wilson, A. D., Clark, V. P., and Witkiewitz, K. (2019). Non-invasive brain stimulation in substance use disorders: implications for dissemination to clinical settings. *Curr Opin Psychol* 30, 6–10. doi:10.1016/j.copsyc.2018.12.009.

Talukdar, S., Owen, B. M., Song, P., Hernandez, G., Zhang, Y., Zhou, Y., et al. (2016). FGF21 Regulates Sweet and Alcohol Preference. *Cell Metab* 23, 344–349. doi:10.1016/j.cmet.2015.12.008.

Thomas, A., Baillie, G. L., Phillips, A. M., Razdan, R. K., Ross, R. A., and Pertwee, R. G. (2007). Cannabidiol displays unexpectedly high potency as an antagonist of CB1 and CB2 receptor agonists in vitro. *Br J Pharmacol* 150, 613–623. doi:10.1038/sj.bjp.0707133.

Torregrossa, M. M., Corlett, P. R., and Taylor, J. R. (2011). Aberrant learning and memory in addiction. *Neurobiology of Learning and Memory* 96, 609–623. doi:10.1016/j.nlm.2011.02.014.

Tournier, B. B., and Ginovart, N. (2014). Repeated but not acute treatment with Δ^9-tetrahydrocannabinol disrupts prepulse inhibition of the acoustic startle: reversal by the dopamine $D_{2/3}$ receptor antagonist haloperidol. *Eur Neuropsychopharmacol* 24, 1415–1423. doi:10.1016/j.euroneuro.2014.04.003.

Uddin, L. Q., Kelly, A. M., Biswal, B. B., Castellanos, F. X., and Milham, M. P. (2009). Functional connectivity of default mode network components: correlation, anticorrelation, and causality. *Hum Brain Mapp* 30, 625–637. doi:10.1002/hbm.20531.

Vandaele, Y., Mahajan, N. R., Ottenheimer, D. J., Richard, J. M., Mysore, S. P., and Janak, P. H. (2019). Distinct recruitment of dorsomedial and dorsolateral striatum erodes with extended training. *eLife* 8, e49536. doi:10.7554/eLife.49536.

Volkow, N. D., Baler, R. D., Compton, W. M., and Weiss, S. R. B. (2014). Adverse Health Effects of Marijuana Use. *New England Journal of Medicine* 370, 2219–2227. doi:10.1056/NEJMra1402309.

Wacker, J., Dillon, D. G., and Pizzagalli, D. A. (2009). The role of the nucleus accumbens and rostral anterior cingulate cortex in anhedonia: integration of resting EEG, fMRI, and volumetric techniques. *Neuroimage* 46, 327–337. doi:10.1016/j.neuroimage.2009.01.058.

Walia, P., Fu, Y., Schwaitzberg, S. D., Intes, X., De, S., Cavuoto, L., et al. (2021). Neuroimaging guided tES to facilitate complex laparoscopic surgical tasks – insights from functional near-infrared spectroscopy. doi:10.21203/rs.3.rs-730076/v1.

Walter, J. T., and Khodakhah, K. (2006). The Linear Computational Algorithm of Cerebellar Purkinje Cells. *J. Neurosci.* 26, 12861–12872. doi:10.1523/JNEUROSCI.4507-05.2006.

Walther, S., and Strik, W. (2012). Motor Symptoms and Schizophrenia. *NPS* 66, 77–92. doi:10.1159/000339456.

Watson, T. C., Obiang, P., Torres-Herraez, A., Watilliaux, A., Coulon, P., Rochefort, C., et al. Anatomical and physiological foundations of cerebello-hippocampal interaction. *eLife* 8, e41896. doi:10.7554/eLife.41896.

WHO | Cannabis *WHO*. Available at: https://www.who.int/substance_abuse/facts/cannabis/en/ [Accessed October 17, 2020].

Wickham, R. J., Park, J., Nunes, E. J., and Addy, N. A. (2015). Examination of Rapid Dopamine Dynamics with Fast Scan Cyclic Voltammetry During Intra-oral Tastant Administration in Awake Rats. *J Vis Exp*. doi:10.3791/52468.

Williams, E.-J., Walsh, F. S., and Doherty, P. (2003). The FGF receptor uses the endocannabinoid signaling system to couple to an axonal growth response. *J Cell Biol* 160, 481–486. doi:10.1083/jcb.200210164.

Windle, M., Gray, J. C., Lei, K. M., Barton, A. W., Brody, G., Beach, S. R. H., et al. (2018). Age sensitive associations of adolescent substance use with amygdalar, ventral striatum, and frontal volumes in young adulthood. *Drug Alcohol Depend* 186, 94–101. doi:10.1016/j.drugalcdep.2018.02.007.

Winklbaur, B., Ebner, N., Sachs, G., Thau, K., and Fischer, G. (2006). Substance abuse in patients with schizophrenia. *Dialogues Clin Neurosci* 8, 37–43.

World Drug Report 2020 *United Nations : World Drug Report 2020*. Available at: //wdr.unodc.org/wdr2020/en/index.html [Accessed October 17, 2020].

Ye, J. C., Tak, S., Jang, K. E., Jung, J., and Jang, J. (2009). NIRS-SPM: statistical parametric mapping for near-infrared spectroscopy. *Neuroimage* 44, 428–447. doi:10.1016/j.neuroimage.2008.08.036.

Yousif, N., Bain, P. G., Nandi, D., and Borisyuk, R. (2020). A Population Model of Deep Brain Stimulation in Movement Disorders From Circuits to Cells. *Front. Hum. Neurosci.* 14. doi:10.3389/fnhum.2020.00055.

Yu, W., and Krook-Magnuson, E. (2015). Cognitive Collaborations: Bidirectional Functional Connectivity Between the Cerebellum and the Hippocampus. *Front Syst Neurosci* 9, 177. doi:10.3389/fnsys.2015.00177.

Zachek, M. K., Takmakov, P., Park, J., Wightman, R. M., and McCarty, G. S. (2010). Simultaneous monitoring of dopamine concentration at spatially different brain locations in vivo. *Biosensors and Bioelectronics* 25, 1179–1185. doi:10.1016/j.bios.2009.10.008.

Zhang, R., and Volkow, N. D. (2019). Brain default-mode network dysfunction in addiction. *NeuroImage* 200, 313–331. doi:10.1016/j.neuroimage.2019.06.036.

Zhang, X., and Santaniello, S. (2019). Role of cerebellar GABAergic dysfunctions in the origins of essential tremor. *PNAS* 116, 13592–13601. doi:10.1073/pnas.1817689116.

Zheng, W., Wang, H., Zeng, Z., Lin, J., Little, P. J., Srivastava, L. K., et al. (2012). The possible role of the Akt signaling pathway in schizophrenia. *Brain Res* 1470, 145–158. doi:10.1016/j.brainres.2012.06.032.

Zimeo Morais, G. A., Balardin, J. B., and Sato, J. R. (2018). fNIRS Optodes' Location Decider (fOLD): a toolbox for probe arrangement guided by brain regions-of-interest. *Scientific Reports* 8, 3341. doi:10.1038/s41598-018-21716-z.